

AD-A106 156

MASSACHUSETTS INST OF TECH LEXINGTON LINCOLN LAB

F/6 9/5

EHF TEST-BED SUBHARMONIC MIXER.(U)

JUL 81 M J AGHION

F19628-80-C-0002

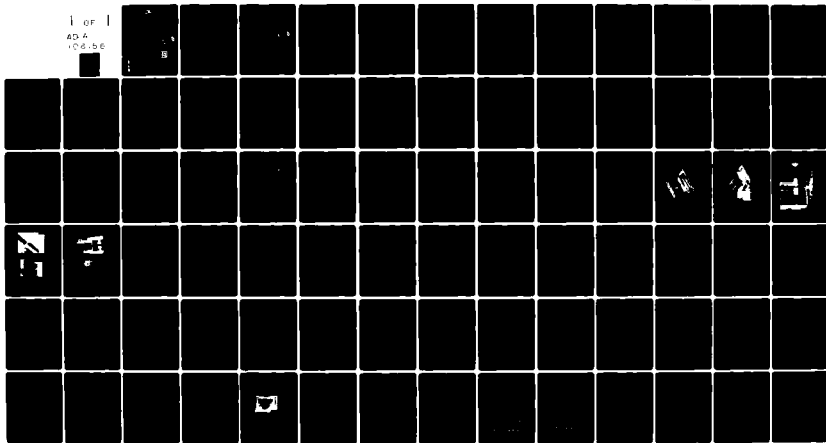
UNCLASSIFIED

TR-567

ESD-TR-81-190

NL

1 of 1
ADA
106-156



END

DATE

FILED

11-81

DTIC

LEVEL

12

AD A106156

Technical Report

567

EHF Test-Bed Subharmonic Mixer

M.J. Aghion

DTIC
ELECTE
OCT 26 1981
S D H

14 July 1981

Prepared for the Department of the Air Force
under Electronic Systems Division Contract F19628-80-C-0008 by

Lincoln Laboratory

MASSACHUSETTS INSTITUTE OF TECHNOLOGY

Lexington, Massachusetts



Approved for public release; distribution unlimited.

FILE COPY

81 10 26 060

The work reported in this document was performed at Lincoln Laboratory, a center for research sponsored by Massachusetts Institute of Technology, with the support of the Department of the Air Force under Contract F19620-60-C-0002.

This report may be reproduced to satisfy needs of U.S. Government agencies.

The views and conclusions contained in this document are those of the contractor and should not be interpreted as necessarily representing the official policies, either expressed or implied, of the United States Government.

This technical report has been reviewed and is approved for publication.

FOR THE COMMANDER

Raymond L. Leisette

Raymond L. Leisette, Lt. Col., USAF
Chief, BED Lincoln Laboratory Project Office

Non-Lincoln Receipts

PLEASE DO NOT RETURN

Permission is given to destroy this document
when it is no longer needed.

12

MASSACHUSETTS INSTITUTE OF TECHNOLOGY
LINCOLN LABORATORY

EHF TEST-BED SUBHARMONIC MIXER

M.J. AGHION
Group 6.1

DTIC
ELECTE
OCT 26 1981
S D H

TECHNICAL REPORT 567

14 JULY 1981

Approved for public release, distribution unlimited

LEXINGTON

MASSACHUSETTS

ABSTRACT

The development, design and construction of a subharmonically pumped mixer at 44 GHz using GaAs Schottky beam lead diodes is discussed. A simplified theory is used to derive a three-port equivalent circuit of the complete mixer which includes effects such as diode parasitics and filter characteristics. Specific design criteria are developed at each of the three mixer signal frequencies, RF, LO and IF, which relate this equivalent circuit to the observed performance.

Accession No.
 THIS CARD
 IS
 TO BE
 USED
 FOR
 IDENTIFICATION
 BY
 DISTRIBUTION/
 APPROVED
 DATE
 1964

CONTENTS

	<u>Page</u>
ABSTRACT	iii
I. INTRODUCTION	1
II. GENERAL DESCRIPTION	2
A. Subharmonic Mixing	2
B. Transmission Medium	2
C. Mixer Description	2
1. Mechanical	2
2. Electrical	3
III. BEAM-LEAD DIODES	6
A. Availability	6
B. Diode Characterization	6
1. Forward I-V	6
2. Reverse I-V	7
3. Diode Equivalent Circuit	7
IV. MIXER EQUIVALENT CIRCUIT	9
A. LO-Stripline Junction	9
B. IF Filter	9
C. LO Filter	10
D. RF Equivalent Circuit	10
E. LO Equivalent Circuit	11
F. IF Equivalent Circuit	12
V. MATHEMATICAL OPTIMIZATION	13
A. Multi-Frequency Circuit	13
B. Optimization Criteria	13
1. Introduction	13
2. Optimization At RF	13
3. Optimization At LO	14
4. Optimization At IF	16
C. Circuit Analysis	17

VI.	MIXER CONSTRUCTION	19
	A. Mixer Body	19
	B. Suspended Stripline Circuit	19
	C. Diode Attachment	20
VII.	OTHER APPROACHES TRIED	21
VIII.	CONCLUSION	22
	APPENDIX I	37
	APPENDIX II	42
	APPENDIX III	45
	APPENDIX IV	50
	APPENDIX V	55
	APPENDIX VI	58
	APPENDIX VII	63
	APPENDIX VIII	68
	ACKNOWLEDGEMENTS	74
	REFERENCES	75

I. INTRODUCTION

The purpose of this writing is to document work undertaken between June 1979 and April 1981 to develop a low noise, subharmonically pumped mixer for a satellite receiver. A further objective is to provide some background and a starting point for future efforts to continue this work.

The main design points are discussed, and although some details may be sketchy, an effort was made to cover all the areas and provide at least the methodology and "flavor" for how the mixer was built. The mixer specifications were:

Signal Band (RF): 43 to 45 GHz (later changed to 43.5 - 45.5 GHz)

Local Oscillator Band (LO): 22.8 to 23.8 GHz

IF: 2.6 GHz

Several mixers were built incorporating different approaches, but the emphasis throughout will be on the latest design since it is considered the one best understood. Some of the others will be briefly mentioned for comparison in section VII.

The best performance achieved in-house was a conversion loss of $10 \text{ dB} \pm 1$ dB over the band. This compares with noise figures around 6-7 dB quoted in the literature; clearly some improvement remains to be achieved. However, it is felt that the full equivalent circuit of the mixer, as developed here, has the potential to predict performance and suggest improvements qualitatively and quantitatively for a broad range of mixer designs in a way that is not explicitly described in the literature researched. As such, this represents one of the fruits of this endeavor.

II. GENERAL DESCRIPTION

A. Subharmonic Mixing

Let RF, LO and IF denote respectively the signal input, local oscillator input and intermediate frequency output of a generalized mixer. For the case at hand, the following relation holds between the frequencies of these signals:

$$IF = n \times LO - RF$$

For a fundamental mixer, $n = 1$; for a subharmonic mixer $n > 1$. The case of interest to us here is for $n = 2$, i.e., the LO frequency used is somehow doubled inside the mixer and the RF frequency then subtracted from it to give the IF. This, rigorously speaking, is a first subharmonic mixer although "first" is usually omitted.

B. Transmission Medium

The transmission medium used in this mixer is called suspended stripline and is shown in Fig. 1 together with the split-block construction and dimensions used. This geometry has been well researched such that dimensions for any realizable impedance may be calculated with confidence^[1]. Appendix V shows the APL program used to determine the transmission line dimensions. The realizable impedances range from 33 ohms to 140 ohms with w going from .085 inch to .002 inch respectively. Larger w than .085 in. may cause short-circuiting with the housing block, while w smaller than .002 in. is hard to reproduce photolithographically.

The dielectric used is quartz or fused silica, with a dielectric constant of 3.78, selected for low loss and good surface smoothness, which is important for low conductive losses in the chrome-gold metalization.

C. Mixer Description

1. Mechanical:

A generalized subharmonic mixer is sketched in Fig. 2 showing its various components; see also Figs. 15, 16. The RF and LO input ports are WR 22 and

WR 42, waveguide respectively. The RF waveguide is of reduced height (.224" x .030") for better coupling to the diodes. Each waveguide input is provided with its own sliding back short, tuned by a micrometer for best response. The IF output port is an SMA coaxial connector.

In between the split-block housing lies a suspended stripline with a quartz substrate strip 2.0" long x 0.134" wide, on which the circuit elements are photolithographically defined. At the IF end, the SMA connector tab (.050 long x .020 wide x .005 thick) is soldered onto the quartz metallization, Fig. 18. At the RF end, two beam-lead diodes .009" square, are thermo-compression (TC) bonded in an anti-parallel configuration across a .012" gap in the conductor. Then, a gold ribbon .030" wide x .0005 thick is TC bonded to the conductor at one end and attached at the other end to the gold plated copper block using a combination of TC and ultrasonic bonding, Figs. 17 and 19. This procedure must provide a good short-circuit path to ground for the diodes, since any series resistance in this path would add directly to the inherent series resistance of the diodes and degrade mixer performance.

2. Electrical:

This mixer concept follows closely those of references [13] and [14]. The operation of the mixer is briefly explained as follows.

The RF signal energy incident from the RF waveguide excites currents in the anti-parallel diode pair, the back short is tuned so that maximum energy transfer (measured as best input match) occurs between the TE_{10} waveguide mode and the TEM mode on the suspended stripline. The LO filter shown in Fig. 2 is a multi-element low pass filter having its cut-off frequency such as to pass the LO and reflect the RF; in our case the cut-off frequency of this filter, f_c , is ≈ 26 GHz. This means that no RF energy may propagate beyond this LO filter, i.e., the RF is terminated reactively. The distance from the diodes to this filter is a critical tuning parameter which is adjusted so that the diodes receive maximum signal power.

The IF filter shown in Fig. 2 is another low pass filter with its cut-off frequency above IF and below LO, chosen here around 10 GHz. The LO power

incident from the LO waveguide onto the stripline will couple to the TEM mode and travel to the right toward the diodes since to the left the IF filter reflects it almost completely. The backshort and position of the IF filter relative to the LO waveguide provide the parameters to maximize this power transfer. The situation is analogous to the common waveguide-to-coax adapter, where excellent transmission can be obtained between the waveguide and TEM modes.

The LO power traveling to the right in Fig. 2, passes through the LO filter with minimal attenuation and reaches the diodes where it must have sufficient amplitude swing to turn them alternatively on and off based on their highly non-linear I-V characteristics. The RF waveguide is cut-off for the LO frequency range, so no LO power will be lost there.

A digression here should be made which relates the subharmonic mixing action with the presence of two anti-parallel diodes^{[4],[6]}: If only one diode were present, it would conduct (turn on) only once during each period of LO oscillation, say during the positive half of the sinusoidal cycle. But if two diodes are anti-parallel, diode A will turn on during the positive half then turn off (reverse-bias) during the negative half, but diode B will turn-on then since it is placed in opposite polarity with A. The result is that this diode pair turns on or conducts twice during each LO oscillation; therefore, the LO frequency for an anti-parallel pair should be halved compared to a fundamental mixer in which the diode arrangement turns on only once per LO cycle. Thus the effective harmonic action of this mixer.

Returning to the mixer operation, we see that the diodes receive the RF and LO signals for mixing (multiplying). The nonlinearity of the diodes will produce an IF and higher order products. The IF signal passes unattenuated through both LO and IF filters to the coaxial output; none of it can propagate in the LO or RF waveguides since they are below cut-off at IF. The image product (image freq = $4 \times \text{LO} - \text{RF}$), which is 48.2 to 50.2 GHz in this mixer, is reflected back to the diodes for further mixing by the LO filter and by an image rejection band-pass filter which is at the RF waveguide. Higher order products such as the sum frequency ($2 \times \text{LO} + \text{RF}$ or 89.6 to 91.6 GHz) cannot be contained due to

moding problems in the stripline and waveguides; the losses they represent will be unavoidable.

III. BEAM-LEAD DIODES

A. Availability:

Finding beam-lead diodes suitable for 44 GHz was somewhat of a problem. The list of possible vendors was limited to Nippon Electric Company (NEC) in Japan, A.E.I. Semiconductors in England, and Alpha Industries, although other places such as Microwave Associates, Hughes and Honeywell-Spacekom had diode projects still in progress which may be completed now.

Of the first three, A.E.I.'s cost was \$100 - \$200 per diode and Alpha's \$400 - \$600, which made it quite expensive to experiment with such devices. NEC's price of \$30 for a slightly lower performance device made it attractive. In fact, when NEC and AEI diodes were placed in the same circuit, no change was observed. This is not a fair comparison of the diodes, of course, since the performance must have been limited by the circuit, but it still indicates that the work could be done with the cheaper NEC diodes #ND5558, until the limit of the device was encountered.

B. Diode Characterization

1. Forward I-V:

An ideal diode has the well-known exponential I-V relation given in (1):

$$I(V) = I_0 \{ \exp [\alpha (V - IR_s)] - 1 \} \quad (1)$$

where

I_0 = diode reverse saturation current

R_s = series resistance

$\alpha = \frac{e}{nkT} = 38.94 \text{ Volt}^{-1}$, at 25°C room temperature if $n = 1$

$n = \frac{38.94}{\alpha}$ = Ideality factor, $n \geq 1$

Using a curve tracer, a set of (I, V) points can be measured and by finding a good curve fit, the parameters I_0 , R_s and n may be found. Appendix I is

the listing of a computer program written in Basic for the Tektronix 4051 to do this function. Typically, a dozen (I, V) points from 10 μ A to 3 mA are taken and the fit is good. Examples and graphs are given in that appendix. As a general practice, I-V data was taken on the diodes again after TC mounting in the circuit to assure that no damage had occurred.

2. Reverse I-V:

Any diode is bound to have some capacitance, C_j , associated with the drift and diffusion of charges in the semi-conductor junction and another, C_p due to the fringing fields around the package and proximity of the anode and cathode leads. If we postulate that C_p is bias-independent, then any component of total capacitance which varies with applied voltage will be considered C_j .

Equation (2) applies to a Schottky junction diode^[2]

$$C(V) = C_{j0} / (1 + V/\phi)^{1/2} + C_p \quad (2)$$

where

- C_p = parasitic package capacitance
- C_{j0} = junction capacitance at 0 bias
- ϕ = quiescent barrier potential of the junction
- V = reverse bias voltage applied
- $C(V)$ = total measured capacitance

By using a 1 MHz capacitance bridge one can measure $C(V)$ for $V = 0$ to 8 Volts or just under reverse breakdown and curve-fit to determine C_{j0} , C_p and ϕ . A numerical example is given in appendix II for a typical NEC diode.

3. Diode Equivalent Circuit

Enough information is now known about the mixer diodes to make a quantitative model or circuit which incorporates the effects of the three parasitic elements R_s , C_j and C_p . The result is shown in Fig. 3.

The topology is consistent with physical insight although slight variations are possible such as placing R_s outside of the C_p connections.

Note that the junction capacitance in Fig. 3 is, strictly speaking, a function of voltage V (eq. 2), with V corresponding to the 10 sinusoidal voltage (the RF voltage being much smaller in this case). However, taking C_j as a constant equal to C_{j0} can be justified as a kind of averaging over one cycle. Fig. 3b represents the ideal exponential diode governed by eq. 2. In a mixer with sufficient LO pumping, $80V_T$ will be alternately cut-off during the forward conduction portion of the LO cycle and very large during reverse bias, so much so that, in either case, the parasitics become negligible and $80V_T$ can be taken as zero or infinite. Both cases are shown in Fig. 4. This is equivalent to taking the diode as an ON-OFF switch operated at the LO frequency. This view is well substantiated in the literature.

If two diodes are connected in an anti-parallel configuration as in a conventional mixer, then one simply parallels the circuits of Fig. 3a and one of Fig. 3b. This is done in Fig. 5, notice that the ideal switch is now actuated at twice the LO frequency, i.e., this is subharmonic pumping. The switch is ON when either diode conducts around the peak value of LO swing. The switch is OFF when both diodes are cut-off while the LO swing is around zero. Note that the parasitics are now worse due to the presence of two diodes. This represents a fundamental drawback of subharmonic mixers compared to conventional diode-mixers in conversion loss and noise figure. If the parasitics are very small, however, this effect may be more than compensated by other factors such as reproducibility and circuit losses.

IV. MIXER EQUIVALENT CIRCUIT

A. LO Stripline Junction

As mentioned previously, the junction of the LO waveguide and the suspended stripline should provide a good match over the LO frequency range. The suspended stripline impedance was chosen to be $90 \pm 120 \Omega$ (conductor width). This choice eased the realization of the IF filter as we will see later.

The problem of an open circuited stripline in a waveguide can be solved analytically. Appendix III gives a listing of a program which can be used to determine the junction dimensions. The example shown corresponds to the test vehicle dimensions. Since the stripline is not open circuited as assumed in the program, one must place the IF filter, which represents a reactive termination for the LO, at the right distance to give an effective open circuit at the strip length reference plane determined in the program.

This junction was tested separately by placing a .018" thick tapered termination made of Eccoworth material in the suspended stripline between the quartz and the copper housing, away from the junction and over the LO filter. The reflected power was thus due solely to the IF filter-stripline-waveguide junction. The results were in excellent agreement with the prediction. One can, therefore, separate the design of this junction from the rest of the mixer and, for the remainder, we will assume that the LO signal has been properly launched on the suspended stripline of 90Ω impedance.

B. IF Filter

This is an 8-element low pass filter of Tchebyshev design having a cut off frequency of 10 GHz, an input impedance of 90Ω to match the LO line and an output impedance of 50Ω compatible with the SMA connector. It is designed in distributed elements using conventional methods and placed at the right distance away from the LO waveguide to give an effective open circuit at the required position in the LO waveguide as mentioned above. Appendix IV gives the APL program used to design this kind of filter.

C. LO Filter

The LO filter is similar to the IF filter. It cuts off at 26 GHz and consists of nine distributed elements with an input and output impedance of 90 ohms. Had a lower characteristic impedance been selected, say 50 ohms, the capacitive sections built in the minimum realizable impedance of 35 ohms would not have had enough capacitance to realize the needed filter values. Also, it was thought that 90 ohms should be closer to the impedance of the RF waveguide and thus provide better coupling to the signal incident on the reduced height WR 22 RF waveguide.

D. RF Equivalent Circuit

Consider the simplified structure of Fig. 6a, showing an anti-parallel diode pair in shunt with a waveguide sliding short. The equivalent circuit of Fig. 6b is easily deduced, where the box represents the equivalent circuit of the diode pair in Fig. 5. If now a LO filter terminated in 90 ohm and a length of 90 ohm line are attached to the diode-pair, the situation is as depicted in Figs. 7a and b. The circuit in Fig. 7b is redrawn in Fig. 8 for clarity after including the diode circuit of Fig. 5.

Figure 8 deserves attention. It incorporates all elements talked about so far in a way that can be examined by linear circuit analysis, optimized, modified or treated in any one of the many ways that linear time-invariant, passive circuits can be treated. It is a network which describes how an RF signal couples to the diodes of the subharmonic mixer, how the filters, parasitics and backshort affect this coupling. In order not to lose sight of our objective, let us examine what happens for the utopian case where the parasitics are zero, the LO filter is perfectly reflective with the phase of a short, and the sliding backshort distance z is tuned exactly for an open circuit to RF. In this case, the circuit of Fig. 8 reduces to that in Fig. 9 where the RF signal sees directly a perfect switch. When the switch is ON, the RF input impedance is zero; when the switch is OFF, the RF input impedance is infinite. Mixer theory [3],[5],[6] shows that minimum conversion loss results when the ratio of RF input impedance

for open and short states (switch is OFF and ON respectively) is maximum, i.e., $r = |Z_{o.c.}|/|Z_{s.c.}|$, is a measure of mixer performance and several formulas relate this ratio r directly to conversion loss^[3] when all other effects are neglected.

In the case of an ideal switch, r is doubly infinite; in the more practical case of Fig. 8 with typical circuit values, r ranges from 22 at RF band edges, 43 and 45 GHz, to 110 at mid-band. Using reference^[3] page 57, this corresponds directly to an optimum conversion loss of 5.6 to 2.6 dB respectively assuming no other imperfections present. These figures indicate a rather high contribution to conversion loss due simply to the circuit topology and the presence of two diodes, roughly doubling the parasitics. The variation in conversion loss of 3 dB across the 2 GHz RF band is close to what is actually measured. We also get an approximate lower bound on conversion loss for this type of mixer. Recall that the best performance observed was a conversion loss of 10 ± 1 dB. The fact that this admittedly simplified analysis can yield nonetheless such realistic numbers simply from the OFF and ON diode states, is an indication that the elements considered in the model are indeed the dominant ones.

E. LO Equivalent Circuit

In the circuit of Figure 8, one can easily see how to incorporate the LO feed network at the end of the LO filter as shown in Fig. 10. Two points should be made here:

1) The LO waveguide to suspended stripline junction was not included since, as mentioned in section IV.A, it is almost "transparent" and does not add substance to the analysis. Therefore, we assume the LO is fed on a TEM suspended stripline mode of 90 ohm impedance from a 90 ohm LO source impedance.

2) The RF waveguide and backshort impedances denoted by Z_g are purely imaginary (inductive) at LO frequencies, since the RF waveguide is below cut off. The waveguide impedance definition used is given as:

$$f > f_c: Z_g = (2b/a) \sqrt{\mu/\epsilon} (\lambda_g/\lambda) \quad (3)$$

$$f < f_c: Z_g = j(2b/a) \sqrt{\mu/\epsilon} (f/\sqrt{f_c^2 - f^2}) \quad (4)$$

Figure 10 depicts the LO-to-diode coupling network which can be analyzed again using conventional circuit analysis such as MARTHA^[15].

F. IF Equivalent Circuit

Only the IF output remains to be incorporated to complete this multi-frequency equivalent circuit of the mixer. It is easy to see that the IF output power is that power which reaches the 90 ohm resistor in Fig. 10, i.e., this is also the IF load. We have assumed that the 90 ohm to 50 ohm transformation done in the IF low pass filter is perfect.

V. MATHEMATICAL OPTIMIZATION

A. Multi-Frequency Circuit

Summarizing the results of the previous discussions, we can draw the circuit block diagram of Fig. 11 where the mixer is completely specified, and the major sub-circuits are conceptually blocked off and labeled for clarity. This representation for the mixer shall be studied in the remainder of this section.

B. Optimization Criteria

1. Introduction

The philosophy adopted here is to judge or compare performance of the mixer by three criteria given qualitatively here as:

- 1) How well the RF "sees" an ideal switching element (compared to the ideal case of Fig. 9).
- 2) How well the LO switches this ideal element.
- 3) How well the IF is matched into its resistive load.

Admittedly it is a great simplification not to consider the non-linear conductance terms of the diode, the harmonic products terminations and numerous other effects. However, including these effects is difficult theoretically, let alone practically, and even this simplified picture provides, as we have seen, more than enough non-idealities to be quite useful.

2. Optimization At RF

We have already described in section IV.D that to minimize conversion loss, $r = |Z_{o.c.}|/|Z_{s.c.}|$ must be maximized. It was found in the many computer circuit analyses done that this condition is quite close to requiring Z_{out} at port 3 of Fig. 11 - looking back toward the RF source - to be matched to the RF generator impedance Z_g . This is intuitively satisfying in that we expect the signal to be somehow matched into the mixer if reflection losses are to be minimized and maximum RF energy converted to IF. Typically the RF port had a return loss around 6 to 10 dB corresponding to a signal loss of 1.2 to .5 dB. This is in

addition to the losses due to the non-ideal switching characteristic mentioned earlier, namely 2.6 to 5.6 dB.

3. Optimization At LO

Considering how well the switch is turned ON and OFF is really a euphemism for the value of the idealized diode's incremental or AC resistance in the forward and reverse bias conditions. This resistance, R_{AC} , can be found by differentiating both sides of an ideal diode I-V characteristic (i.e., eq. 1 with $R_s = 0$) with respect to I, the result is:

$$R_{AC} = \frac{dV}{dI} = 1/\alpha I(V) \quad (5)$$

Equation 5 shows that the larger I, the smaller the resistance for the switch when it is turned ON. If the LO power is sufficiently high, R_{AC} will be low for the forward conduction and large for the reverse bias. However, LO power available is not unlimited so it is desirable to efficiently couple it to the diode for "hard" switching.

One may be tempted to optimize the match of the LO signal into the mixer. However, the switch ideally absorbs no power in either state, so if the LO is being absorbed efficiently into the mixer, it is probably being dissipated in resistive elements like R_s and thereby reducing the switching efficiency. A better objective should be to maximize the "available power" between the LO source at port 2 and the switch at port 3 in Fig. 11. This criterion is independent of whether the switch can or cannot dissipate any power, it is rather a combination of the short-circuit current flowing through the switch when it is ON and the open-circuit voltage at the switch when OFF. A derivation of this parameter follows.

Figure 12 shows a signal generator of impedance Z_g . In our case, this represents the LO source with a pure real 90 ohm characteristic impedance. The maximum available power P_{av} (Max) from this source is

$$P_{av} \text{ (Max)} = \frac{1}{4} \text{Re} (V_{o.c.} \times I_{s.c.}^*) \quad (6)$$

where $V_{o.c.} = V_g$ = open circuit voltage of the generator (7)

and $I_{s.c.} = \frac{V_g}{Z_g}$ = short circuit of the generator (8)

Substituting (7) and (8) in (6) we get the well known result

$$P_{av} (Max) = \frac{1}{4} \frac{|V_g|^2}{R_g} \quad (9)$$

If now a mixer circuit, such as that of Fig. 11, is placed between the LO source and the ideal switch as in Fig. 13 we must find the new $V'_{o.c.}$ and $I'_{s.c.}$ at the output port 3 where the primes are used to distinguish these from the quantities in eqs. 7 & 8 at the input port 2. At port 3 we have:

$$P_{av} = \frac{1}{4} \text{Re} (V'_{o.c.} \times I'^*_{s.c.}) \quad (10)$$

The ratio of P_{av} to $P_{av} (Max)$ is the quantity desired, from (10) and (6):

$$\eta \equiv \frac{P_{av}}{P_{av} (Max)} = \text{Re} \frac{V'_{o.c.}}{V_{o.c.}} \times \frac{I'^*_{s.c.}}{I_{s.c.}} = \text{Re} (OCVG \times SCCG^*)$$

where OCVG and SCCG denote respectively the open-circuit-voltage-gain and the short-circuit-current-gain of the network in Fig. 13. For this passive circuit as expected, it is always true that:

$$0 \leq \eta \leq 1 \quad (11)$$

Note that either OCVG or SCCG may be greater than 1 but η will still obey eq. 11.

The LO-feed design in the mixer was adjusted to maximize η . This was done by modifying the first five elements of the 9-element LO low pass filter beyond their standard Tchebyshev values by trial and error on the computer. These elements are on the end of the filter nearest the LO waveguide, Fig. 2, so that the rejection of the RF frequencies at the other end of the filter was

practically unaffected. The value of η achieved in the circuit model was around 0.85 (0.7 dB) over the 1 GHz LO band. The corresponding LO output impedance seen by the switch at port 3 in Fig. 11 - looking toward the LO 90 ohm load - was around $(13-j 4)$ ohm over the band. This corresponds to a mismatch or reflection loss of 3.5 dB which is very large indeed. The observed LO reflections from the mixer were of this same order.

Measurements of conversion loss for input LO drives up to + 13 dBm showed no bottoming off relative to LO drive, which indicates poor LO coupling, Fig. 14. These observations may mean that, instead of η , a better objective after all is to match the circuit output impedance at LO to improve performance. However no easy way was found to do so in this circuit topology.

On another level, it is interesting to speculate whether this parameter η could be used instead to optimize the RF coupling into the diodes, rather than r of section IV D. It is suspected, however, on the basis of sketchy calculations that both r and η should behave similarly, and which would be the better choice could not be determined without a complete analysis.

4. Optimization At IF:

Assuming that the LO pumps the diode switch efficiently and that the RF energy reaches this switch with minimum losses, the mixing function will take place and all intermodulation products $P_{m,n}$ will be produced as given by:

$$P_{m,n} = n \times \text{LO} \pm m \times \text{RF} \quad (12)$$

where m and $n = 0, 1, 2, \dots$

Of these, the higher order terms, with $m + n$ large, contain little signal energy and cannot be controlled in any case so we will write them off as some small loss (< 2 dB). Those with $m > 1$ are negligible since they vary as the RF energy (small) raised to the $|m|$ th power which is smaller still. The term $2 \text{ LO} - \text{RF}$ is the IF for the case at hand. Another notable term, $4 \text{ LO} - \text{RF}$, is the image frequency (48.2 - 50.2 GHz). It is reflected by the LO filter and the guide bandpass filter located at the RF input back to the diodes for another mixing, yielding an addition to the IF signal. If the phase of this IF contribution

matches the directly generated IF, then some "image enhancement" occurs^{[7],[8]} which reduces the mixer conversion loss.

Assuming all these mechanisms take place, we should then consider how the IF signal generated at the switching diode-pair is captured by the external IF load (90 ohms). This is the LO situation in reverse. Again, if the ratios of available powers at the switch terminals (port 3 in Fig. 11) and at the IF load (port 2 in Fig. 11) are close to 1, the IF power is being transferred out of the mixer efficiently.

Therefore, one can use η of the previous section at the IF band as well. When this is done, η at 2.6 GHz is 0.7 corresponding to 1.6 dB less IF power available than generated. This contributes directly to conversion loss and should be added to the two previous contributions. No effort was made to adjust any IF filter elements to raise η . For these conditions, the output IF impedance seen from the switch at port 3 in Fig. 11 looking back toward the IF load was $(72 - j 21) \Omega$ compared to the optimum value of 90Ω .

C. Circuit Analysis

We have stated several times that the study of the mixer was reduced to the analysis of a conventional equivalent circuit. In fact, in the past discussion, figures of impedance, efficiency, etc., were quoted freely. In this section we outline how these figures were obtained. The complete listings of the three programs involved are given in appendix VI together with the run from which the figures came and which represents the best performance achieved.

The circuit analysis was done by MARTHA and APL functions. The procedure is briefly as follows:

A given set of LO filter dimensions are chosen as designed by the function in Appendix V.

As mentioned in section V.B.3 the first five elements are adjusted to maximize η . The function LPF59 is next called with the modified dimensions as arguments. A MARTHA network called SPLOLPF is created to represent this LO filter.

Next the function BS is called with some more dimensions such as ℓ_1 and ℓ_2 of Fig. 8. BS defines the mixer equivalent circuit by properly wiring SPLOLPF with all other blocks of Fig. 11. Since the full equivalent circuit is a three-port device, it is convenient to have two separate networks:

- 1) for the LO and IF with input at port 2 and output at port 3 (the switch) with the RF port terminated in the RF waveguide impedance. This one is called LONET and
- 2) for the RF with input at port 1, output at port 3 and $90\ \Omega$ termination at port 2. This one is called RFNET. It is emphasized that LONET and RFNET are simply different orientations of the same 3-port circuit, they are needed only for the MARTHA convenience of analyzing 2-port networks.

The last function PT is now called to calculate the various performance criteria discussed in relation to LONET and RFNET. The important results of such a calculation are given in appendix VI.

VI. MIXER CONSTRUCTION

A. Mixer Body

The mixer body was machined out of Tellurium-Copper which combines high conductivity and good machining properties. The body photographed in Figs. 15, 16 is seen to be made of a single lower half and a split top half. Without this split the long waveguide channels, especially the .030" high one, could not be machined with normal lengths cutters. To insure good contact between the top and bottom halves the lower half is pocketed or undercut to reduce the area of contact and confine it close to the quartz substrate. The shelf in the lower half where the .010" thick quartz substrate drops, had to be held within .001" otherwise excessive looseness of the substrate could break the ribbon contact or cause intermittence. Locating pins also required similar tolerance. All other dimensions were usually adequate with $\pm .002$ " allowance. After machining, a patch of thick gold plating was deposited to allow TC and ultrasonic bonding of a gold ribbon, Fig. 17.

B. Suspended Stripline Circuit

A quartz wafer measuring 2" x 1" x .010" is used to deposit up to seven circuits, each .134" wide with a gap of .004" in between circuits. These gaps account for the thickness of the diamond-impregnated saw used to slice the wafer into individual circuits. The circuits are defined photolithographically using a computer controlled package "MANNPLOT" and a pattern generator. See Appendix VIII.

Typically the circuits on the same wafer are identical except for one or two parameters (e.g., ϵ_2 of Fig. 8) which differ in typically .005" steps. Then they can be tested in the body to find the best one. The circuit metallization consists of a thin layer of chromium followed by gold. Poor adhesion of the metallization on the quartz was noticed occasionally especially on small conductor patches. However, good metallization process control solves the problem. At the IF end of the substrate, the SMA connector tab is soldered onto the metallization as shown in Fig. 18.

C. Diode Attachment

No operation was more critical than the attachment of two diodes side-by-side on a fragile .010" thick ceramic surface. Good temperature and pressure settings of the TC bonding wedge tip are essential. The issue of providing a short to ground (the body) at the diode is also a thorny problem. The ribbon solution although somewhat "inelegant" is satisfactory. Figure 19 shows a 100X blow-up of a particularly successful assembly.

VII. OTHER APPROACHES TRIED

Several other designs were investigated with little success compared to the finally adopted one which was discussed here. They are mentioned here briefly for completeness.

One such approach is depicted in Fig. 20 where the diodes are mounted in shunt with the TEM suspended stripline. This was done following references [9] to [12]. The problem of grounding the diodes is now found at two different locations, and no solution was found before this topology was abandoned.

Another variation attempted is shown in Fig. 21. Here the shunt geometry is still used but the short circuit to ground is attempted using three quarter-wave open-circuited stubs for the LO, RF image and even the sum frequency ($2LO + RF = 88.6$ to 92.6 GHz). A large DC block chip capacitor (> 50 pF) was used to provide a short-circuit to ground at IF and allow external biasing of the diodes. This scheme had a high conversion loss and its intricate assembly discouraged further trials.

The test set-up used in all measurements mentioned is described in Appendix VII.

VIII. CONCLUSION

A subharmonic mixer in the low millimeter-waves has been presented. The various elements were examined step by step in a somewhat heuristic approach, starting from a single diode to an anti-parallel pair to their mounting in the signal waveguide to the LO feed network to the IF output. All these elements were then incorporated in a three-port equivalent circuit representing the mixer. Straightforward ways to analyze this circuit were deduced based on mixer theory and other physical arguments. This was done over each of the frequency ranges of interest, namely RF, LO and IF.

The case of the best mixer built was described in some detail and the theoretical conversion loss-predicted using the equivalent circuit model-ranges from 4.7 to 8.4 dB^{*} compared to a measured 9 to 11 dB. The discrepancy reminds us of other neglected mechanisms such as conductive RF losses, non-zero switch resistance in the ON state due to insufficient LO power coupling, other fringing or parasitic elements not included in the circuit etc.

Finally, the important question of how to improve future mixer performance should be addressed. Here, one can only propose tentative ideas since if any of them were sure to succeed they would have been tried earlier.

In view of the millimeter wave frequencies, the involved machining and the uncertainty in circuits and element values, an important objective would be to break up the mixer into smaller parts more easily analyzed. One such part would be the RF waveguide-diode-LO filter junction. If a single diode were used and some external DC bias were introduced to turn this diode ON and OFF, some network analyzer measurements could be made at RF to determine $Z_{o.c.}$, $Z_{s.c.}$ and refine the equivalent circuit as well as optimize it on this structure. Then, accounting for the second diode as well as the rest of the elements could proceed on a sounder basis.

* The non-ideal switching contributed 2.6 to 5.6 dB; the RF input mismatch 0.5 to 1.2 dB; the IF mismatch 1.6 dB.

A similar measurement could be made at IF on a structure like the one above but augmented with the IF filter. This filter could then be modified to improve the IF-to-diode coupling.

The problem of LO coupling to the diodes should be re-examined. Perhaps the LO filter should be left with standard Tchebyshev elements or, if modified, then step by step and with actual measurements to determine whether each step made an improvement or not.

The performance criteria developed here would remain applicable in carrying out the ideas for the further work mentioned above.

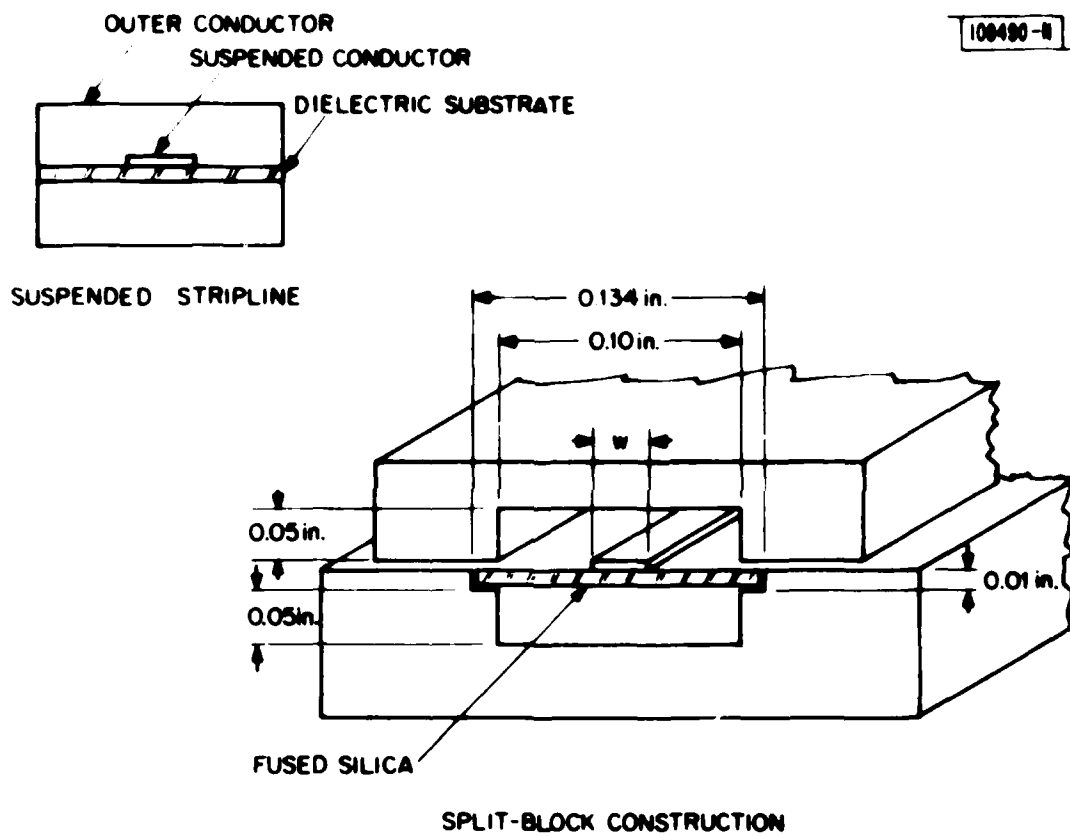


Fig. 1. Suspended stripline geometry and dimensions.

109405-N

TUNABLE SLIDING SHORT-CIRCUITS

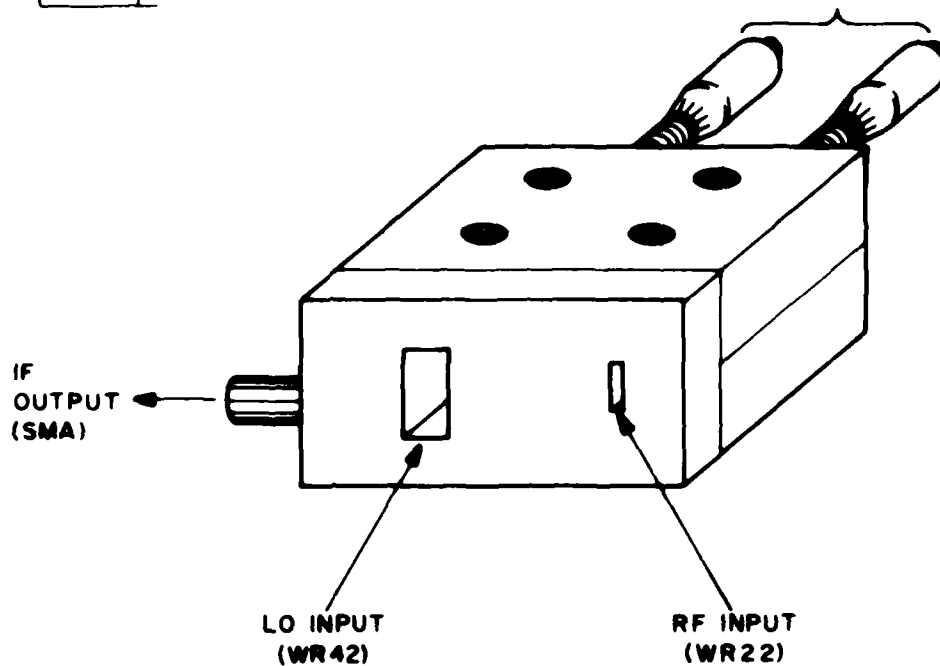


Fig. 2a. Subharmonic mixer assembly.

109406-N

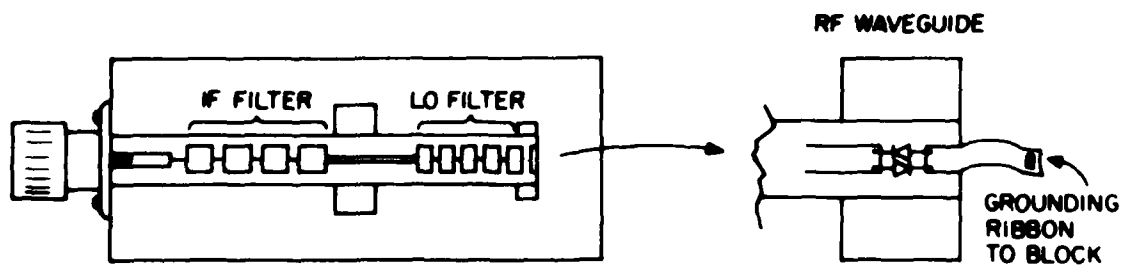


Fig. 2b. Subharmonic mixer substrate assembly.

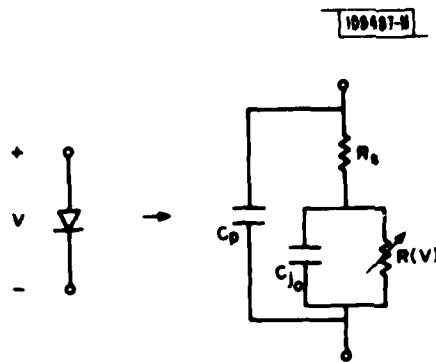


Fig. 3. Beam-lead mixer diode and equivalent circuit.

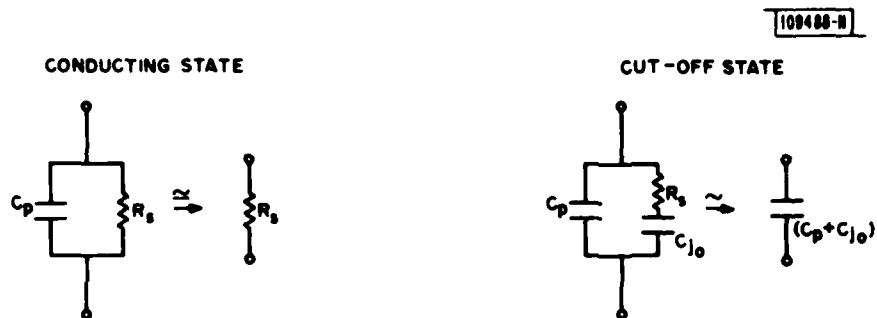


Fig. 4. Diode circuit, a) in forward bias and b) in reverse bias.

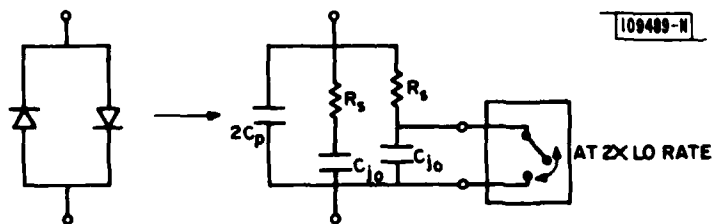


Fig. 5. Anti-parallel diode pair and circuit.

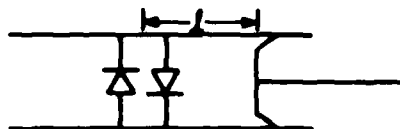


Fig. 6a. Diode pair in waveguide with backshort.

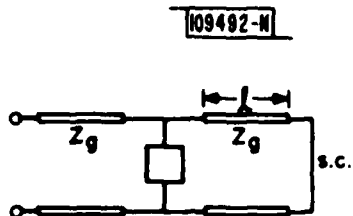


Fig. 6b. Equivalent circuit of structure in Fig. 6a.

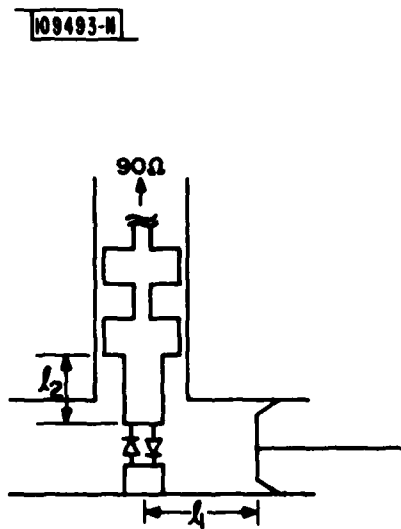


Fig. 7a. Diode pair in waveguide with LO filter.

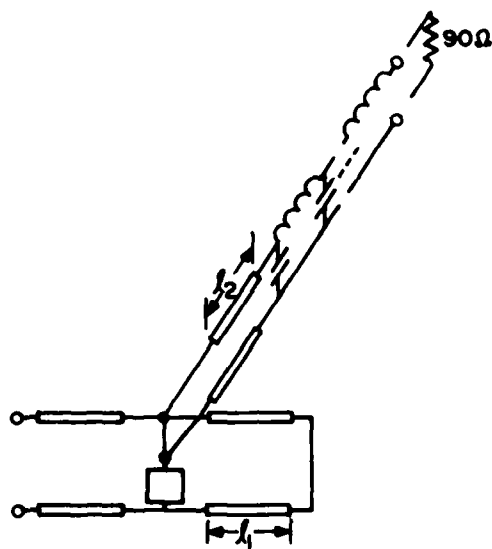


Fig. 7b. Equivalent circuit of structure in Fig. 7a.

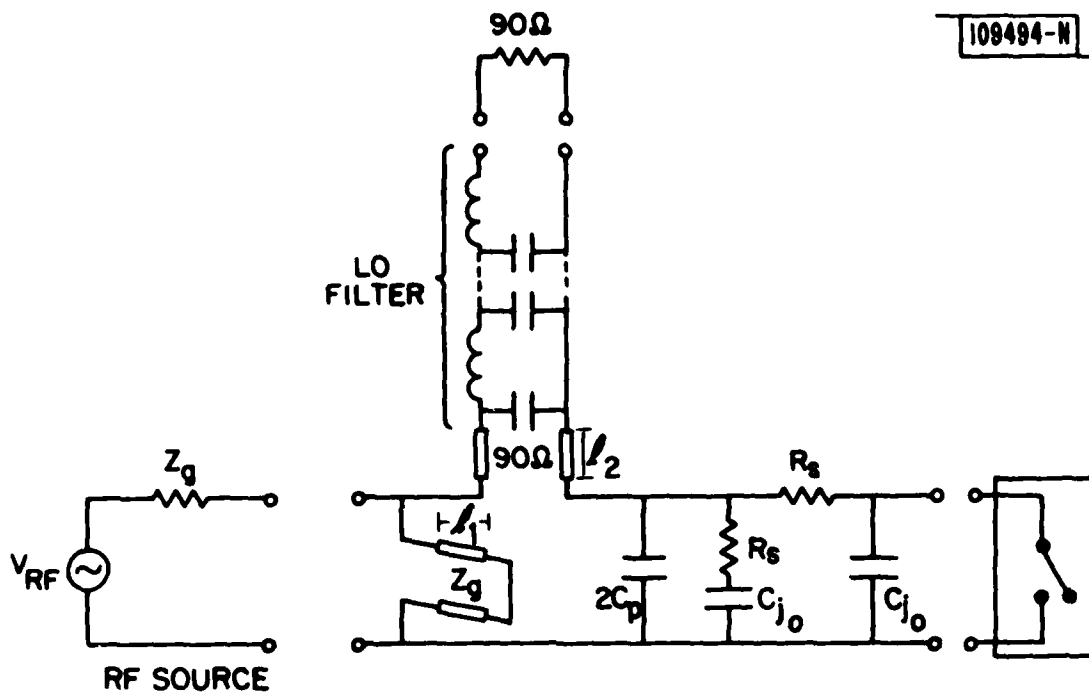


Fig. 8. Mixer equivalent circuit at RF.

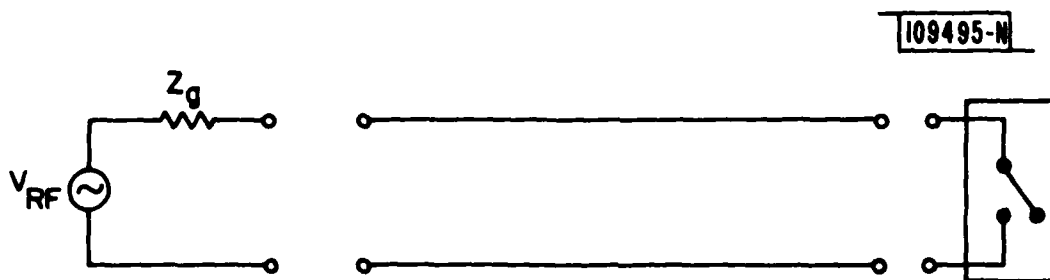


Fig. 9. Idealized case of mixer at RF.

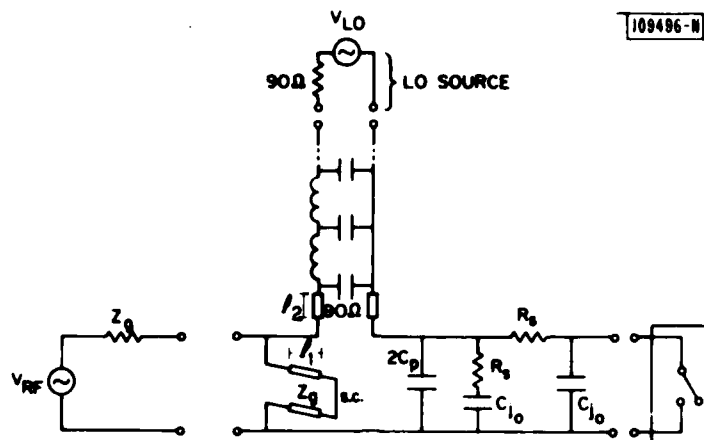


Fig. 10. Mixer equivalent circuit at RF and LO.

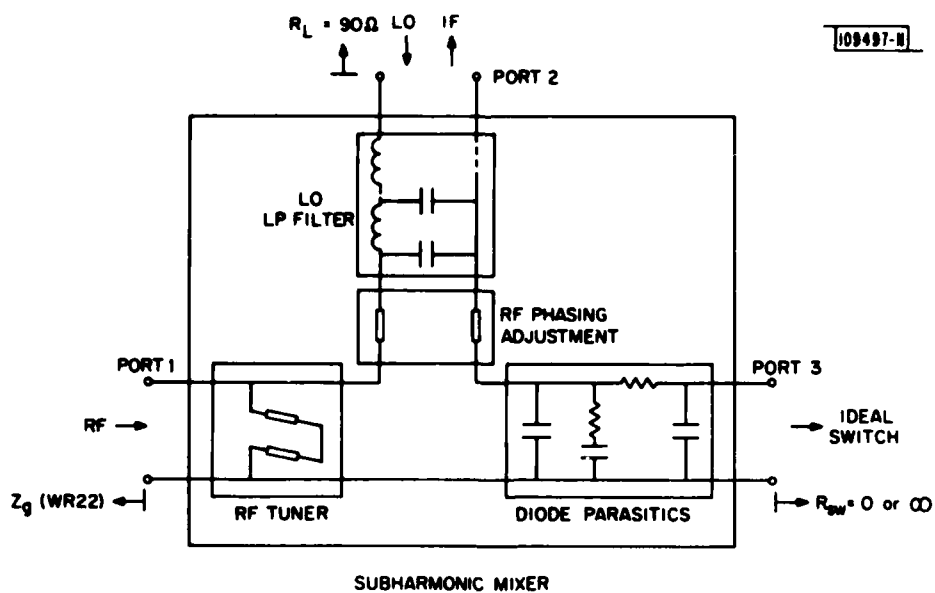


Fig. 11. Complete 3-port mixer equivalent circuit.

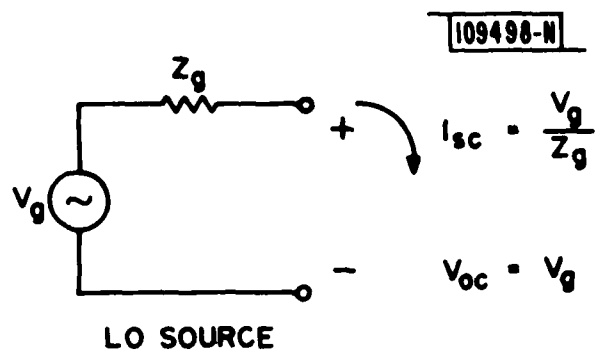


Fig. 12. Model of LO pump source.

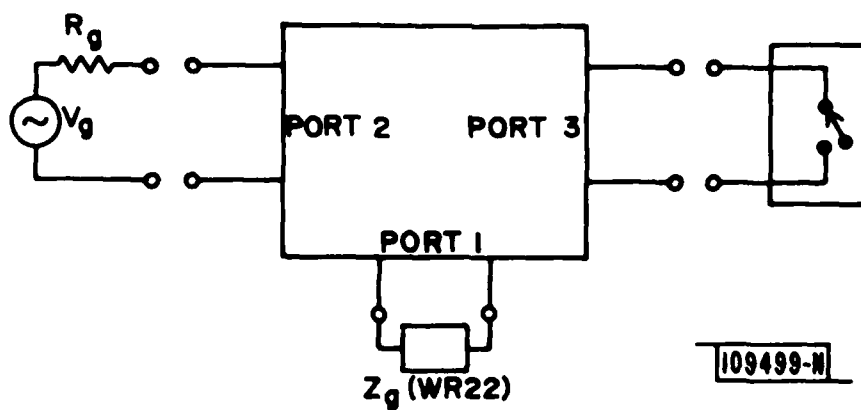


Fig. 13. Mixer circuit for LO to diode coupling.

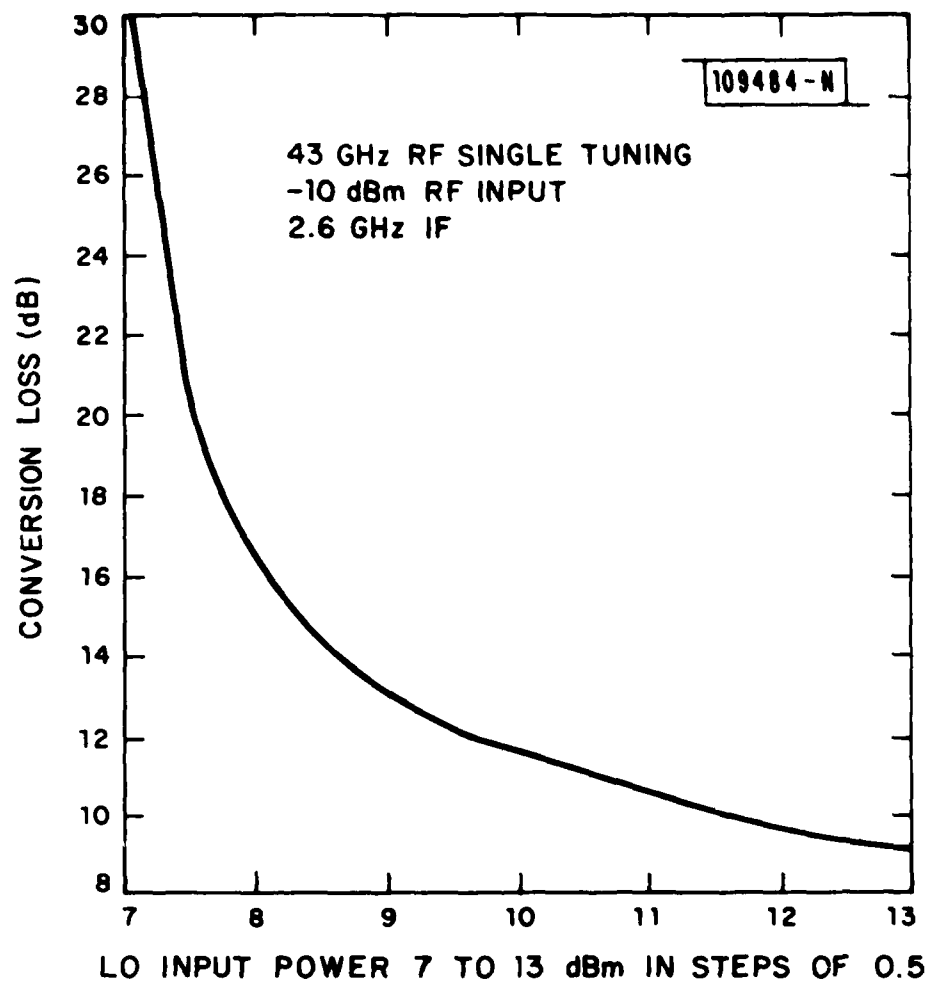


Fig. 14. Conversion loss versus available LO pump power.

109505-S

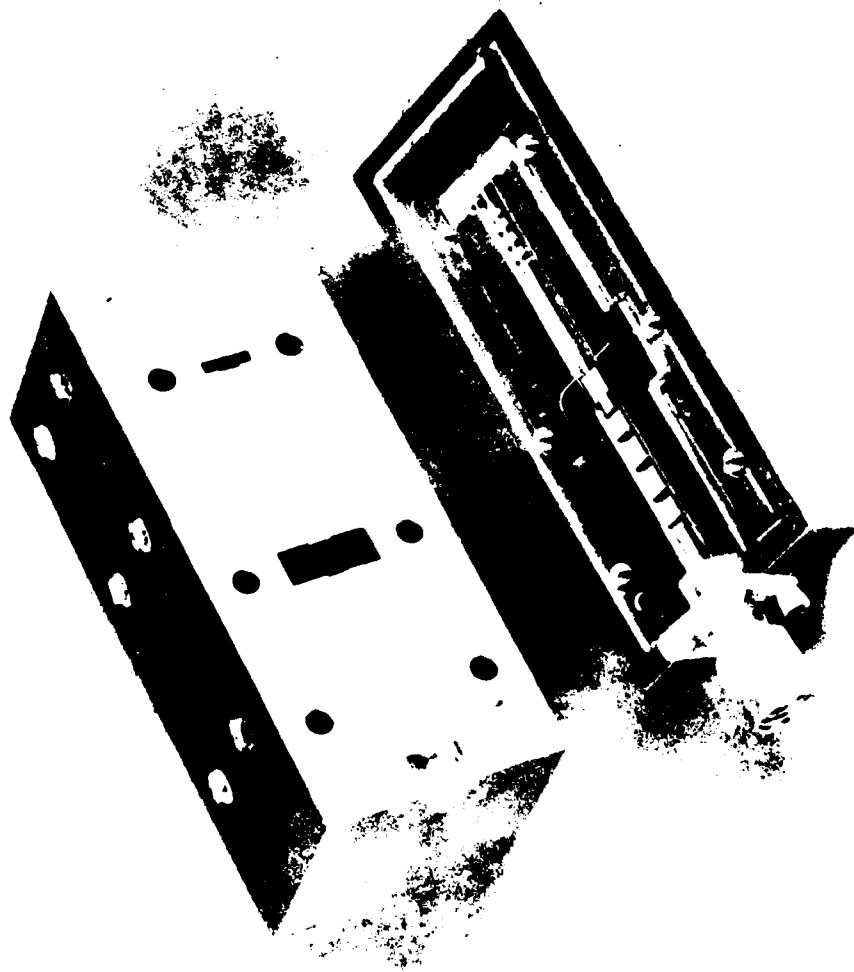
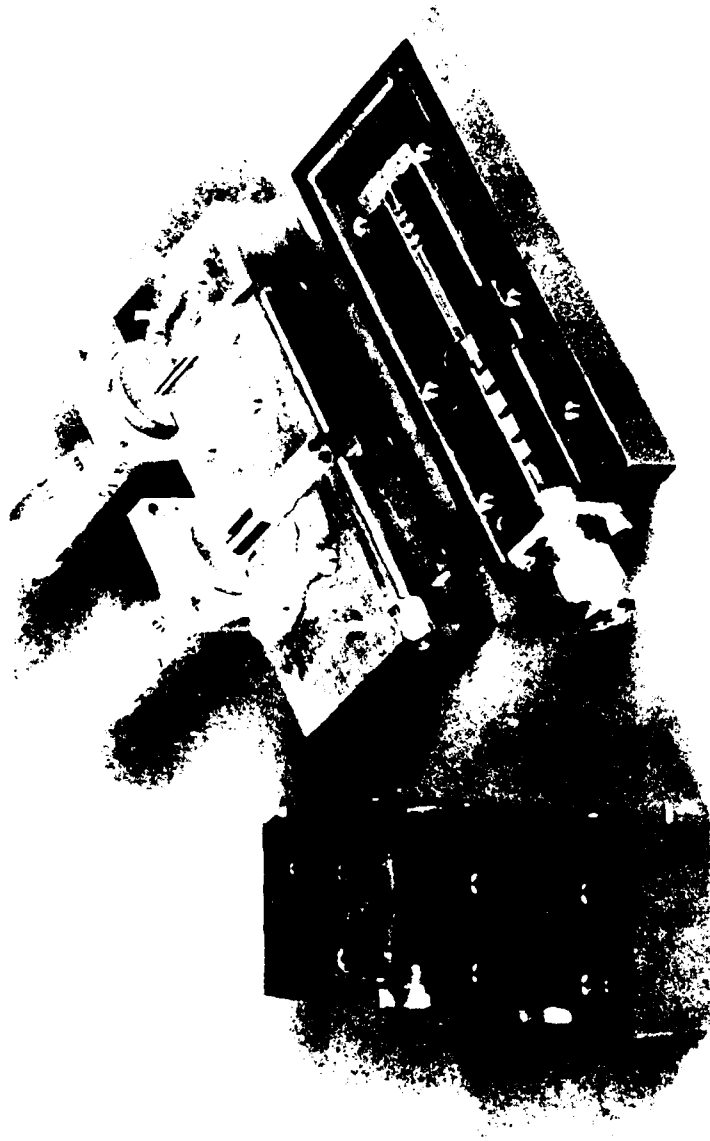


Fig. 15. Mixer body showing both halves.



109506-S

Fig. 16. Mixer body showing three pieces.



Fig. 17. Diode pair mounted in RF waveguide.



Fig. 18. Solder junction of SMA to suspended stripline.

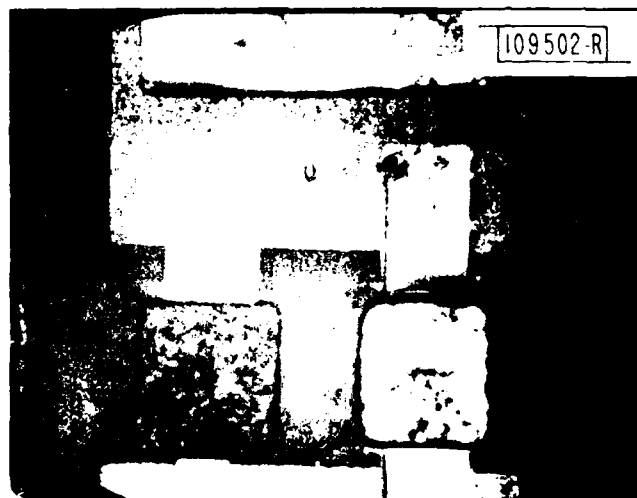


Fig. 19. Detail of mounted diodes.

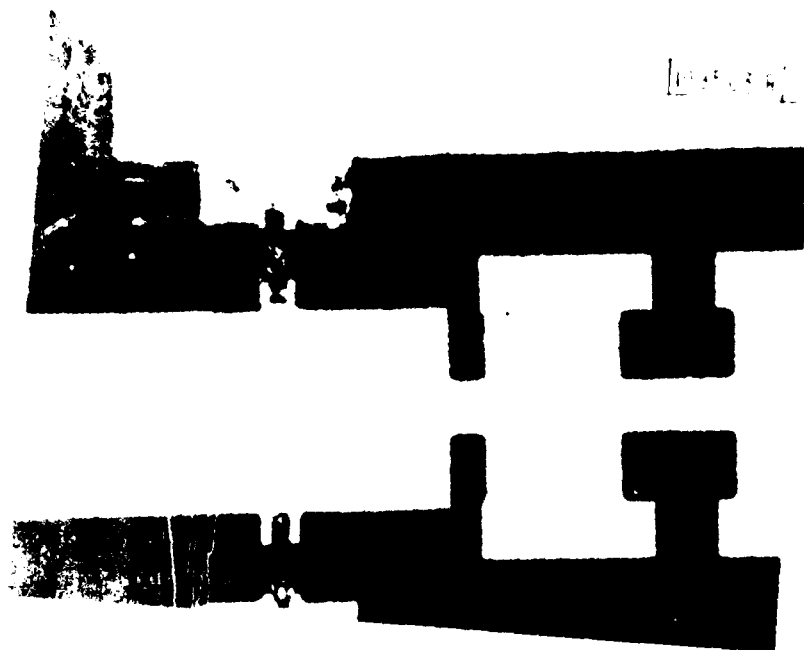


Fig. 1. Drive part mounted in shunt with stripline.

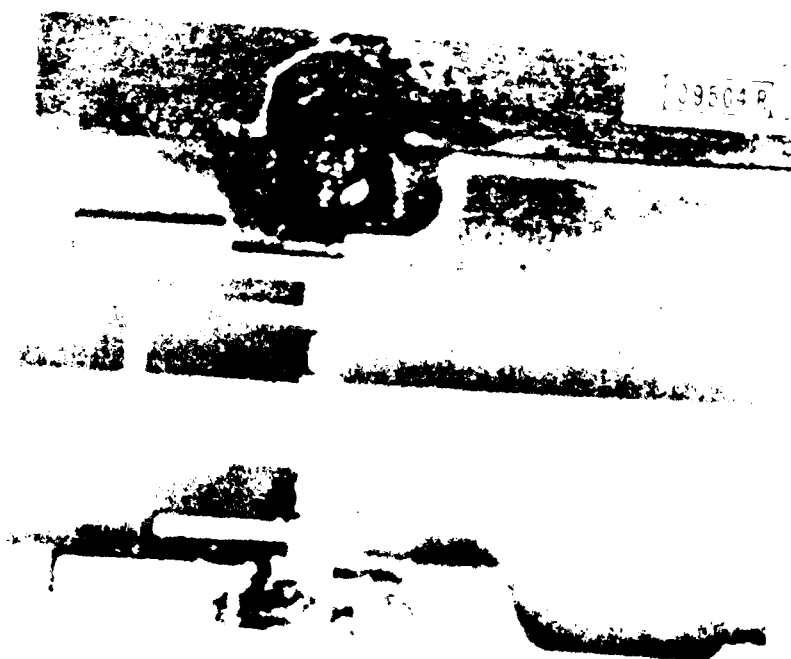


Fig. 2. Drive part mounted in shunt with stubs for virtual ground.

APPENDIX I

This is a listing of a Basic program which determines α , I_o and R_s from a set of (I-V) points taken by a curve tracer.

The examples given are typical of the diode ND5558.

F

```

PROGRAM TO DETERMINE DIODE PARAMETERS
FROM A SET OF THREE (I,U) POINTS

110 DIM U(3,20),A(20),I(20),R(20)
100 PRINT "ENTER (I1,U1) , (I2,U2) , (I3,U3) IN AMPS AND VOLTS"
110 INPUT I1,U1,I2,U2,I3,U3
120 E=1.0E-4
130 R(1)=0
140 FOR N=2 TO 20
150 A(N)=LOG(I2/I1)/(U2-U1-R(N-1)*(I2-I1))
160 I(N)=I3/(EXP(A(N)*(U3-R(N-1)*I3))-1)
170 I(N)=1/3*(2*I1/(EXP(A(N)*(U1-R(N-1)*I1))-1)+I(N))
180 R(N)=(U3-LOG(I3/I(N)+1)/A(N))/I3
190 U(1,N)=LOG(I1/I(N)+1)/A(N)+R(N)*I1
200 U(2,N)=LOG(I2/I(N)+1)/A(N)+R(N)*I2
210 U(3,N)=LOG(I3/I(N)+1)/A(N)+R(N)*I3
220 IF ABS(U(1,N)/U1-1)>E OR ABS(U(2,N)/U2-1)>E THEN 240
230 GO TO 250
240 NEXT N
250 PRINT A(N),I(N),R(N),N,U(1,N),U(2,N),U(3,N)
260 PRINT "ENTER ANY I GET CORRESPONDING U"
270 INPUT I0
280 U0=LOG(I0/I(N)+1)/A(N)+R(N)*I0
290 PRINT "I=",I0," U=",U0
300 GO TO 270
310 STOP

```

```

run
ENTER (I1,U1) , (I2,U2) , (I3,U3) IN AMPS AND VOLTS
30e-6, .565, .25e-3,.625, 2.5e-3,.710
36.658978733 3.063260289E-14 9.84891537601 9
0.565024738147 0.625028995515 0.71
ENTER ANY I GET CORRESPONDING U
1e-3
1= 1.0E-3 U= 0.670231638981

```

.004
I= 0.737594342046
.010
I= 0.021682022257

U=
U=

0.004
0.01

PROGRAM ABORTED IN LINE 270

alpha = 36.65 or $n=38.94/\alpha$ pha=1.062
izero = 3.06e-14 ampere
series resistance = 9.8 ohms

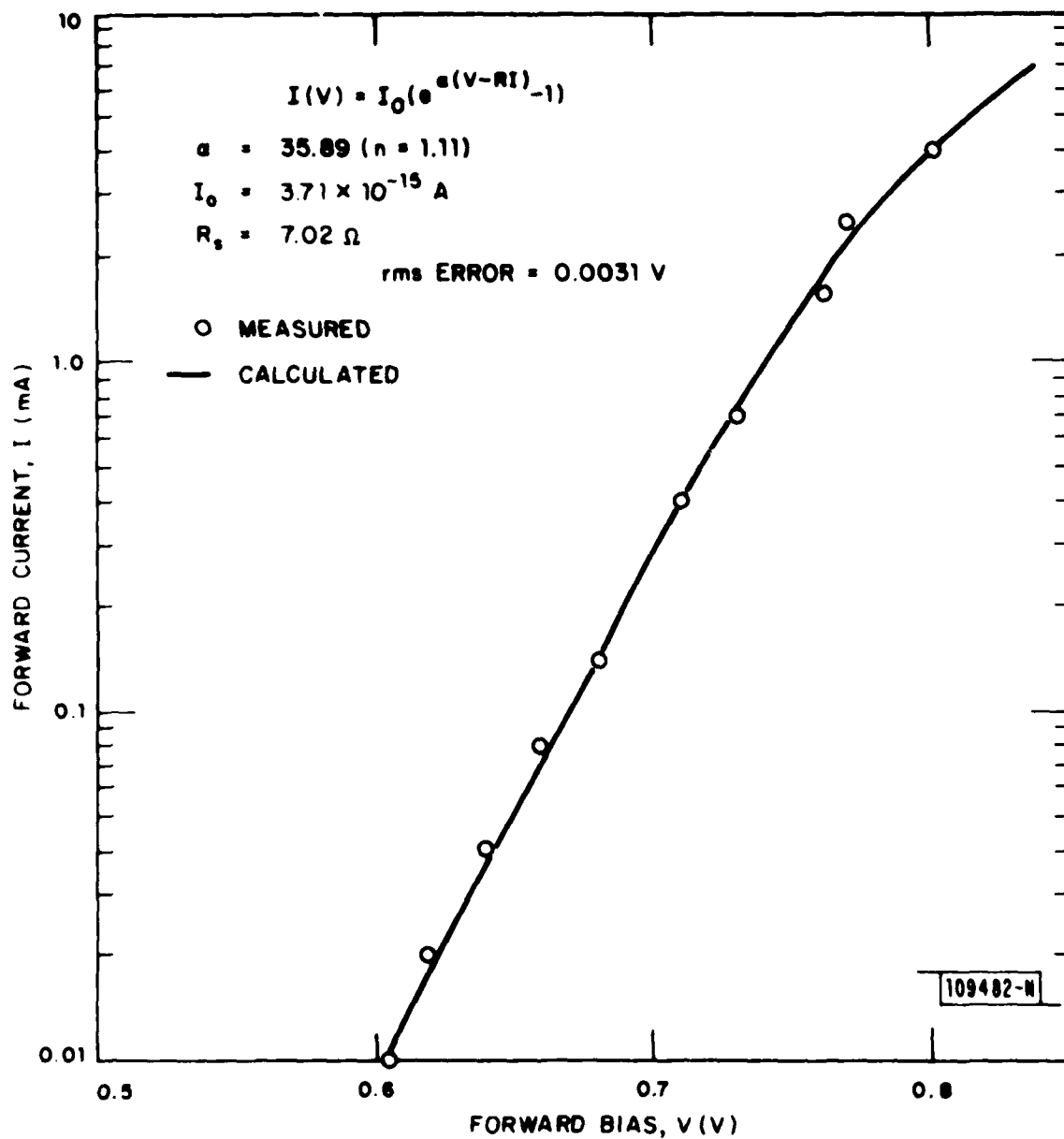


Fig. I-1. NEC ND5558 diode forward current vs voltage.

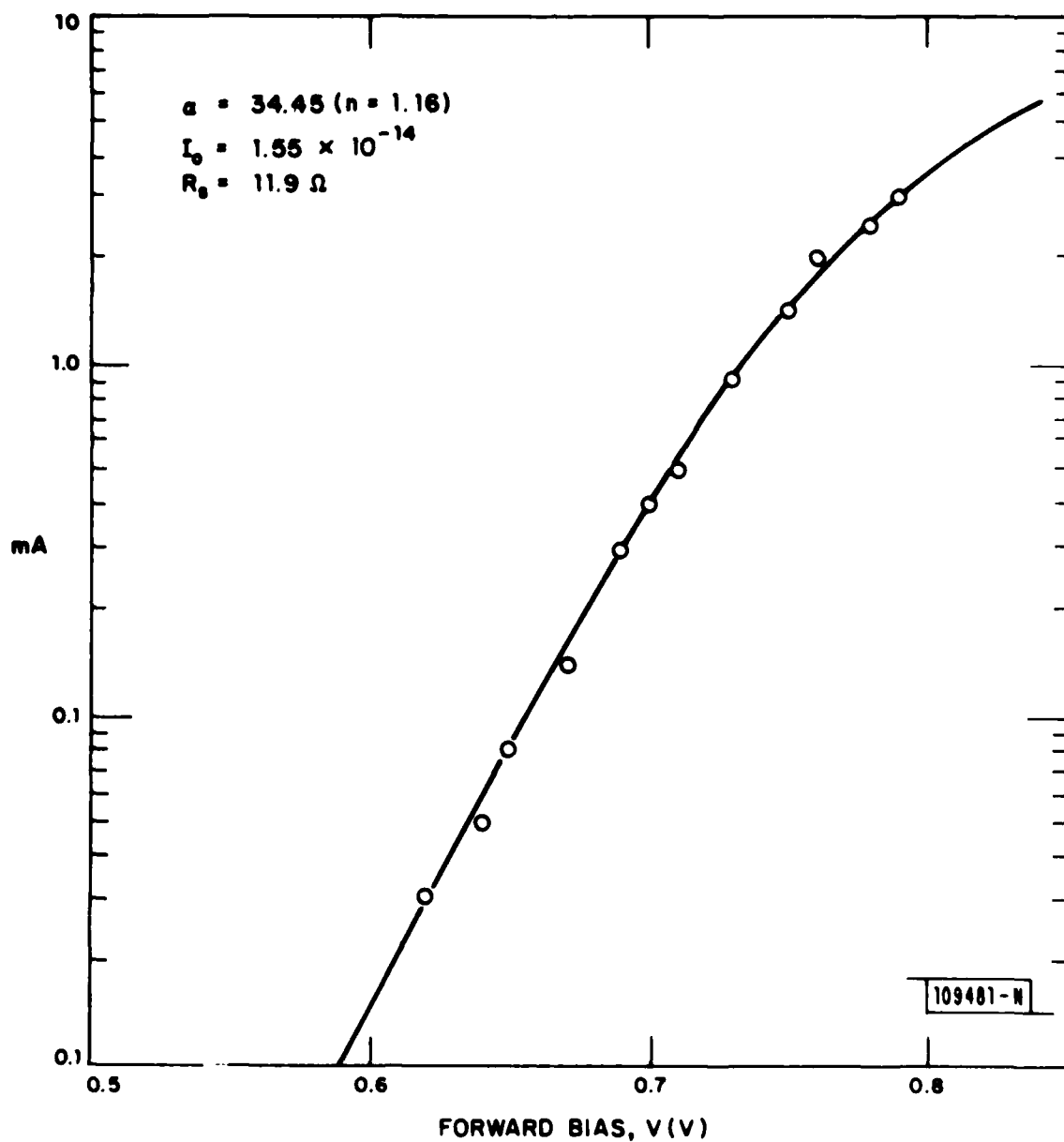


Fig. I-2. NEC ND5558 diode forward current vs voltage.

APPENDIX II

A typical set of C-V points taken on a 1 MHz programmable capacitance bridge of a NEC ND5558 beam-lead Gallium-Arsenide Schottky diode is shown in Fig. II-1.

Also shown in the figure are the extracted equivalent circuit parameters by curve-fitting.

NEC DIODES, 37-2-2, 1/2/1980

V	C(V)	S(V)	1/C(V)^2
0.0	0.124	-0.063	6.470E 01
0.3	0.117	-0.058	7.290E 01
0.5	0.114	-0.060	7.734E 01
0.8	0.109	-0.071	8.450E 01
1.0	0.106	-0.061	8.945E 01
1.3	0.103	-0.067	9.446E 01
1.5	0.101	-0.059	9.785E 01
1.8	0.098	-0.059	1.040E 02
2.0	0.098	-0.058	1.049E 02
2.3	0.097	-0.057	1.055E 02
2.5	0.095	-0.059	1.099E 02
2.8	0.095	-0.058	1.101E 02
3.0	0.093	-0.057	1.148E 02
3.3	0.093	-0.049	1.165E 02
3.5	0.092	-0.045	1.184E 02
3.8	0.092	-0.040	1.170E 02
4.0	0.092	-0.031	1.179E 02

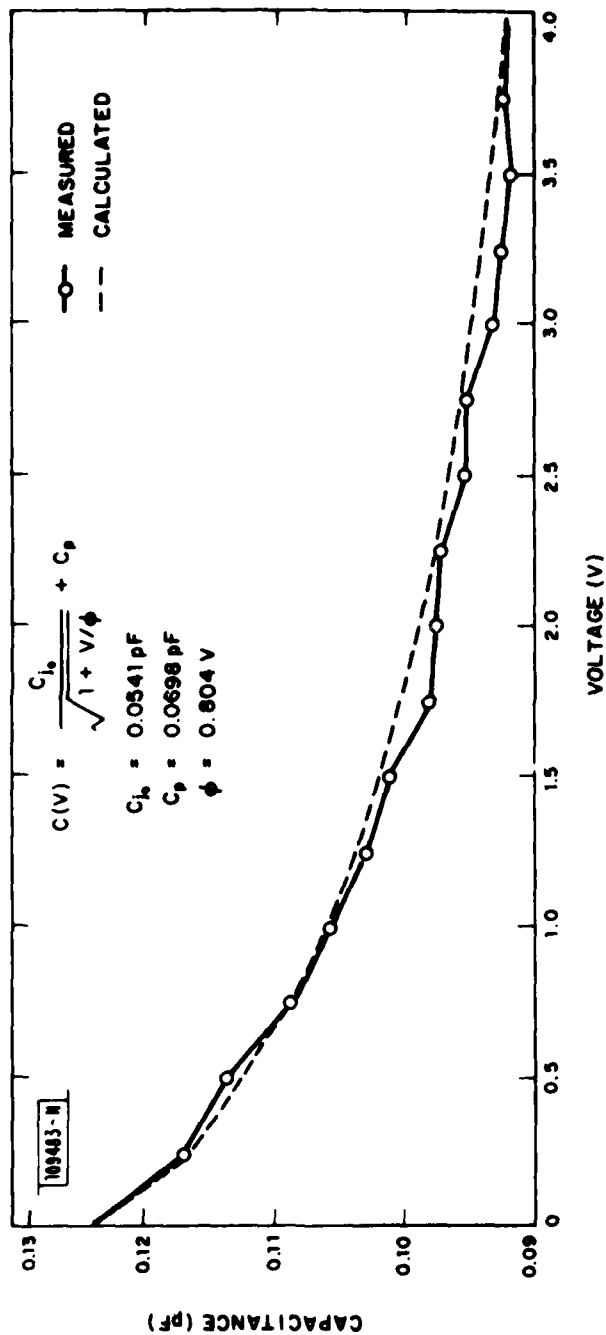


Fig. II-1. NEC ND558 diode capacitance vs voltage.

APPENDIX III

This is a listing of the Basic program to model and design a waveguide to stripline junction.

It was used to determine the dimensions of the LO waveguide-stripline junction and position of the IF filter.

WAVEGUIDE TO SUSPENDED STRIPLINE JUNCTION MODEL
USED TO FIND DIMENSIONS OF BEST MATCH

```

11st
80 REM TO FIND REAL AND IMAGINARY PARTS OF INPUT IMPEDANCE OF STRIP
90 REM TO WAVEGUIDE ADAPTOR
94 P0=0
100 PRINT "ENTER A AND B DIMENSIONS OF WAVEGUIDE (ALL DIMS IN INCHES)"
110 INPUT A,B
120 PRI "ENTER IMPEDANCE OF TEM LINE USED IN RETRN LOSS CALCULTN ONLY"
125 INPUT R0
127 PRI "ENTER SERIES INDUCTOR IN NH (SUCH AS DUE TO STEP)FOR SAME CALC"
128 INPUT H0
130 PRINT "ENTER SHUNT CAPACITOR IN PF DUE TO JUNCTION DISCONTINUITY"
131 INPUT C0
137 PRINT "ENTER RELATIVE EFFECTIVE DIELECTRIC CONST. OF STRIP IN GUIDE"
138 INPUT E
140 PRINT "ENTER START AND STOP FREQUENCIES AND NUMBER OF POINTS WANTED"
150 INPUT F1,F2,N1
160 PRI "ENTER MAXIMUM M AND N FOR SUMMATION OVER TE AND TM (M,N)MODES "
170 INPUT M0,N0
180 PRINT "ENTER W AND D; WIDTH AND LENGTH OF THIN STRIP IN WAVEGUIDE"
190 INPUT W,D
200 PRINT "ENTER L DISTANCE TO SHORT-CIRCUIT IN BACK OF STRIP"
210 INPUT L
220 PRI "FREQUENCY RE(ZIN) IM(ZIN) IM(Z0) NET X R.L.DB I.L.DB"
230 IF N1>1 THEN 260
240 F=F1
250 GO TO 270
260 FOR F=F1 TO F2 STEP (F2-F1)/(N1-1)
270 L0=11.803/F
280 K=2*PI/L0*SQR(E)
290 G0=L0/SQR(1-(L0/(2*A))^2)
300 N=2/(PI*K*W)*SQR(2*A/B)*SIN(PI*W/(2*A))*TAN(K*D/2)
310 R=377*N*2*G0/L0*SIN(2*PI*L/G0)^2

```

```

320 X1=R/TAN(2*PI*L/G0)
330 X2=377*2/(PI*SIN(K*D))^12
340 IF P0=0 THEN 380
350 PRINT " REAL PART ZIN,      X1,      X2<MULTIPLIER OF SUMMATION>"
360 PRINT R,X1,X2
370 PRINT "      M      N      X(M,N)"
380 S=0
390 FOR M=1 TO M0
400 E1=2
410 FOR N=0 TO N0
420 E2=2
430 IF N>0 THEN 460
440 E2=1
450 IF M=1 THEN 560
460 K1=SQR((M*L0/(2*A))^12+(N*L0/(2*B))^12-1)
470 U=SIN(M*PI/2)*SIN(M*PI*M/(2*A))
480 V=U*(COS(K*D))-COS(N*PI*D/B))
490 W=U/((N*PI)^12*M/(K*B^12)-K*M)
500 U=(E1*E2/K1-K1*(2*A/B*N/M)^12)/(M^12*B/A+N^12*A/B)
510 X3=U*X0^12
520 IF P0=0 THEN 550
530 PRINT M,N,X3
540 PRINT E1,E2
550 S=S+X3
560 NEXT N
570 NEXT M
580 X=X1+X2*S
582 T0=2*PI*F*R0*C0/1000
585 X0=2*PI*F*H0-R0*T0/(1+T0^12)
587 R1=R0/(1+T0^12)
590 U0=0.5*SQR((SQR(R/R1)+SQR(R1/R))^12+(X+X0)^12/(R*R1))
600 I0=8.686*LOG(U0)
610 I1=-4.343*LOG(1-1/U0^12)
620 PRINT USING 630:F,R,X,X0,X+X0,I1,I0
622 PRINT R1

```

```

6300 IMAGE 2X,2D,2D,3X,4D,1D,3X,4D,1D,3X,4D,1D,4X,4D,1D,5X,2D,1D,3X,2D,2D
6400 IF N1=1 THEN 660
6500 NEXT F
6600 PRI "ENTER: 4 TO CHNG L ONLY: 3 FOR W,D,L; 2 FOR M,N,F,W,D,L; 1 FRO"
6700 INPUT N2
6800 IF N2=4 THEN 200
6900 IF N2=3 THEN 180
7000 IF N2=2 THEN 160
7050 IF N2=1 THEN 710
7070 PRINT "WHAT !!!!!!!?????????"
7100 PRINT "ENTER START AND STOP FREQUENCIES AND NUMBER OF POINTS WANTED"
7200 INPUT F1,F2,N1
7300 GO TO 220
7400 STOP

```

```

RUN
ENTER A AND B DIMENSIONS OF WAVEGUIDE (ALL DIMS IN INCHES)
.420 .170
ENTER IMPEDANCE OF TEM LINE USED IN RETRN LOSS CALCULTN ONLY
90
ENTER SERIES INDUCTOR IN NH (SUCH AS DUE TO STEP)FOR SAME CALC
0
ENTER SHUNT CAPACITOR IN FF DUE TO JUNCTION DISCONTINUITY
0
ENTER RELATIVE EFFECTIVE DIELECTRIC CONST. OF STRIP IN GUIDE
1.2
ENTER START AND STOP FREQUENCIES AND NUMBER OF POINTS WANTED
20.8 25.8 11
ENTER MAXIMUM M AND N FOR SUMMATION OVER TE AND TM (M,N)MODES
3 3
ENTER W AND D; WIDTH AND LENGTH OF THIN STRIP IN WAVEGUIDE
.020 .125
ENTER L DISTANCE TO SHORT-CIRCUIT IN BACK OF STRIP

```

```

.140
FREQUENCY RE(ZIN) IM(ZIN) IM(ZO) NET X R.L.DB I.L.DB
20.80 72.1 7.9 0.0 7.9 18.4 0.06
90
21.30 75.7 7.1 0.0 7.1 20.3 0.04
90
21.80 79.3 6.2 0.0 6.2 22.7 0.02
90
22.30 82.7 5.0 0.0 5.0 25.8 0.01
90
22.80 86.1 3.8 0.0 3.8 30.2 0.00
90
23.30 89.3 2.3 0.0 2.3 37.4 0.00
90
23.80 92.5 0.7 0.0 0.7 37.1 0.00
90
24.30 95.5 -1.0 0.0 -1.0 30.4 0.00
90
24.80 98.5 -2.8 0.0 -2.8 26.5 0.01
90
25.30 101.3 -4.7 0.0 -4.7 23.9 0.02
90
25.80 104.1 -6.7 0.0 -6.7 21.9 0.03
90
ENTER:4 TO CHNG L ONLY; 3 FOR W,D,L; 2 FOR M,N,F,W,D,L; 1 FRQ

```

PROGRAM ABORTED IN LINE 670

APPENDIX IV

This is a listing of the APL program used to design low pass filters in suspended stripline medium using high and low impedance lines as distributed elements.

```

V LIND[0] V
  V LNGTH=LIND L
  [1] →(1+MC=L+Z1)/MAX
  [2] LNGTH←(U1+MC)×10MC=L+Z1
  [3] →RETURN
  [4] MAX:LNGTH←(U1+MC)×1.5708
  [5] RETURN: V

  V LCAPI[0] V
  V LNGTH=LCAPI C
  [1] →(1+Z2=MC=C+1000)/MAX
  [2] LNGTH←(U2+MC)×10Z2=MC=C+1000
  [3] →RETURN
  [4] MAX:LNGTH←(U2+MC) 1.5708
  [5] RETURN: V

  V INDOF[0] V
  V LNH=INDOF LNGTH
  [1] LNH←(Z2+MC)×30(MC=LNGTH+2×U2) V

  V CAPOF[0] V
  V CPF=CAPOF LNGTH
  [1] CPF←(1000+Z1+MC)×30(MC=LNGTH+2×U1) V

  V LSTEP[0] V
  V LNH=LSTEP 0
  [1] LAMBDA←11.883+FC
  [2] LNH←(2+0[3]+MC)×(0[1]+2×(02)×B+01)+LAMBDA
  [3] LNH=LNH←0+1008.5×0[3]+0[2] V

  V PROTOG[0] V
  V G=N PROTOG RPL:B
  BETA←0+70RPL+17.37
  GAMMA←50BETA+2×N
  K←1N
  [1] A=100((2×K)-1)+2×N
  [2] B←(GAMMA+2)÷(100K+N)=2
  [3] G←K,N+1,8
  [4] G[1]←2×A[1]+GAMMA
  [5] I←1
  [6] LOOP:→(N-I)/LASTG
  [7] I←I+1
  [8] G[I]←4×A[I-1]=A[I]+B[I-1]×G[I-1]
  [9] →LOOP
  [10] LASTG:→(0-N-2×(N+2))/NEVEN
  [11] G[N+1]←1
  [12] →SUM
  [13] NEVEN:G[N+1]←(70BETA+4)×2
  [14] SUM:G[N+2]←÷((N+1),0.0)/G
  [15] V

```

```

V LPF101
V LPF X
[1] 'ENTER IMPEDANCE, EFF DIEL, STRIP WIDTH-FOR INDUCTIVE THEN CAPACITIU
E LINES'
[2] X=X,0
[3] 'ENTER STRIPLINE DIMENSIONS A,W,H1(0 O.K.),H2,H3,DIEL, FRING CAP IN
PF/CM, EXTRA C IN PF'
[4] X=X,0
[5] WC=0.2*FC*X[11]
[6] B=X[14]*X[15]*X[16]
[7] U1=11.803*(E1+X[7])*0.5
[8] U2=11.803*(E2+X[10])*0.5
[9] G=((N+1),0,0)/(N+X[2]) PROTOG(RPL+X[3])
[10] L=((Z0+X[4])*WC)*G
[11] C=((1000+Z0*WC)*G)-X[19]
[12] Z1=X[6]
[13] Z2=X[9]
[14] LNGTHL=LIND 0.8*L
[15] LNGTHC=LCAP 0.5*C
[16] W0=X[13]
[17] W1=X[8]
[18] W2=X[11]
[19] CD1=2.54*2*X[18]*W2-W0
[20] CD2=2.54*2*X[18]*W2-W1
[21] LD1=LSTEP W0,(Z1),Z0
[22] LD2=LSTEP W2,Z1,Z2
[23] LD3=LSTEP W2,Z0,Z2
[24] 'JUNCTION SERIES INDUCTANCE IN NH, (L TO Z0):(L TO C):(Z0 TO C)'
LD1,LD2,LD3
[25] 'EDGE SHUNT CAPACITANCE IN PF, (C TO Z0): C TO L'
CD1,CD2
[26] I=((2*N)+1)*(N)/(2*N)+1
[27] J=((2*N)+N)/2*N
[28] M=0
[29] M=0
[30] M=0
[31] + (IND,CAP)[X[5]]

```

```

[61] 'ELEMENT LENGTHS (0 MEANS NO EL
      EMENT)', INDUCTORS FIRST, 1

[32] IND:LNGLTHL←N*0
[33] LNGLTHL[J]←0
[34] LNGLTHC[1,I,N]←0
[35] REPEAT1:M←M+1
[36] LNGLTHL[1]←LIND L[1]-LD1+LD2+INDOF LNGLTHC[2]
[37] →((0+N-2*(N+2)),0-N-2*(N+2))/LODD,LEVEN
[38] LODD:LNGLTHL[N]←LNGLTHL[1]
[39] →CYCLE1
[40] LEVEN:LNGLTHC[N]←LCAP C[N]-CD1+CD2+CAPOF LNGLTHL[N-1]
[41] LNGLTHL[N]←0
[42] CYCLE1:LNGLTHC[J]←LCAP C[J]-(2*CD2)+(CAPOF LNGLTHL[J-1])+(CAPOF LNGLTHL[J
+1]
[43] LNGLTHL[I]←LIND L[I]-(2*LD2)+(INDOF LNGLTHC[I-1])+(INDOF LNGLTHC[I+1]
[44] →((M<4),M≥4)/REPEAT1,OUTPUT
[45] CAP:LNGLTHC[J]←0
[46] LNGLTHL←N*0
[47] LNGLTHL[1,I,N]←0
[48] REPEAT2:M←M+1
[49] LNGLTHC[1]←LCAP C[1]+(1000*LD3+Z0*2)-CD1+CD2+CAPOF LNGLTHL[2]
[50] →((0+N-2*(N+2)),0-N-2*(N+2))/CDD,CEVEN
[51] CDD:LNGLTHC[N]←LNGLTHC[1]
[52] →CYCLE2
[53] CEVEN:LNGLTHL[N]←LIND L[N]-LD1+LD2+INDOF LNGLTHC[N-1]
[54] LNGLTHC[N]←0
[55] CYCLE2:LNGLTHL[J]←LIND L[J]-(2*LD2)+(INDOF LNGLTHC[J-1])+(INDOF LNGLTHC[J
+1]
[56] LNGLTHC[I]←LCAP C[I]-(2*CD2)+(CAPOF LNGLTHL[I-1])+(CAPOF LNGLTHL[I+1]
[57] →(M<7)/REPEAT2
[58] OUTPUT: INPUTS: FC, N, RIPPLE, Z0, 1ST ELEM(1=IND,2=CAP),(ZIND,EIND,M
IND),(ZCAP,ECAP,WCAP),A, W, H3(TOP), H2, H1, D
      IEL'
[59] 'FRINGING APACITANCE OF LINE IN PF/CM (FROM SMITH PROG), EXTRA CAPAC
      ITANCE IF ANY IN PF'
[60] X

```

```

[61] 'ELEMENT LENGTHS (0 MEANS NO ELEMENT), INDUCTORS FIRST, 1 TO N'
[62] LENGTHL
[63] LENGTHC
[64] 'MAXIMUM ACHIEVABLE ELEMENT LENGTHS : INDUCTORS, CAPACITORS-'
[65] (1.5708*U1*WC), (1.5708*U2*WC)
[66] 'OVERALL FILTER LENGTH IN INCHES:'
[67] +/LENGTHL,LENGTHC

LPF 10 8 0.4 90 2
ENTER IMPEDANCE, EFF DIEL, STRIP WIDTH-FOR INDUCTIVE THEN CAPACITIVE LINES
0:
140 1.87 .002 35 1.5 .085
ENTER STRIPLINE DIMENSIONS A,W,H1(0 O.K.),H2,H3,DIEL, FRING CAP IN PF/CM,
EXTRA C IN PF
0:
.100 .020 .020 .010 .020 3.78 .057 0
JUNCTION SERIES INDUCTANCE IN NH, (L TO Z0):(L TO C):(Z0 TO C)
0.01698666216 0.09707024943 0.05617409034
EDGE SHUNT CAPACITANCE IN PF, (C TO Z0): C TO L)
0.0188214 0.02403348
INPUTS: FC, N, RIPPLE, Z0, 1ST ELEM(1=IND,2=CAP),(ZIND,EIND,WIND),(ZCAP,EC
AP,WCAP),A, W, H3(TOP), H2, H1, DIEL
FRINGING APACITANCE OF LINE IN PF/CH (FROM SMITH PROG), EXTRA CAPACITANCE
IF ANY IN PF
10 8 0.4 90 2 140 1.87 0.002 35 1.5 0.085 0.1 0.02 0.02 0.01 0.02 3.78 0.0
57 0
ELEMENT LENGTHS (0 MEANS NO ELEMENT), INDUCTORS FIRST, 1 TO N
0 0.08484517195 0 0.08833594075 0 0.08703649842 0 0.05963107363
0.07663248128 0 0.1239377229 0 0.127022968 0 0.1169115524 0
MAXIMUM ACHIEVABLE ELEMENT LENGTHS : INDUCTORS, CAPACITORS-
0.2157807151 0.240928292
OVERALL FILTER LENGTH IN INCHES:
0.7643534093

```

APPENDIX V

This is a listing of the APL functions used to calculate the impedance of the suspended stripline given its dimensions.

```

[1]  COEF [0]
[2]  X0+A COEF B;K;E1;E3;W1;U1;U2;X0
[3]  E1-E3+1
[4]  N-1A
[5]  H1=O(A[5]+A[1])×N
[6]  H2=O(A[4]+A[1])×N
[7]  H3=O(A[3]+A[1])×N
[8]  S1=5OH1
[9]  S2=5CH2
[10] S3=5OH3
[11] C1=6CH1
[12] C2=6CH2
[13] C3=6OH3
[14] NN=E1×C1×S2+A[6]×S1×C2
[15] EN=(E1×C1×C2)+A[6]×S1×S2
[16] DN=(A[6]×EN×S3)+E3×NN×C3
[17] GN=(A[1]×NN+ODN×N)×S3
[18] W1=O(A[2]+2×A[1])×N
[19] SH=10W1
[20] CW=2CH1
[21] U1=(4+ON)×(100N+2)×SW
[22] U2=(2×A[2]+A[1])×(100N+2)×(SW+W1)+(3+W1×2)×(20W1)+(2×SW+W1)+(10W1+
[23] 2)×W1+2)×2
[24] K1=GN×(4×U2)-U1
[25] K=(+/K1×U1)++/K1×U2
[26] UN=(U1+K×U2)+A[2]
[27] X0=(2×(1+K+4)×2)+A[1]×+/GN×UN+2

```

7 SUSUB [0] 7 88.12849084 0.7955217203 1.580141271

7 X0-A SUSUB A

[1] X1+2
[2] 376.62+((C+A COEF X1)*C+A COEF(5*X1),1)*0.5
[3] U+(C+Q)*0.5
[4] 0-2*U,1+U*2
[5] IMPEDANCE OHMS
[6] 7
[7] EFFECTIVE DIELECTRIC CONSTANT
[8] U*2
[9] FREE SPACE CAPACITANCE/LENGTH
[10] C
[11] EFFECTIVE CAPACITANCE/LENGTH
[12] 7

100 SUSUB .100 .053 .020 .010 .020 3.78
IMPEDANCE OHMS

50.2798036
EFFECTIVE DIELECTRIC CONSTANT

1.448546225
FREE SPACE CAPACITANCE/LENGTH

6.223629015
EFFECTIVE CAPACITANCE/LENGTH

9.015212868
50.2798036 0.8308714202 1.448546225

100 SUSUB .100 .020 .020 .010 .020 3.78
IMPEDANCE OHMS

88.12849084
EFFECTIVE DIELECTRIC CONSTANT

1.580141271
FREE SPACE CAPACITANCE/LENGTH

3.399688199
EFFECTIVE CAPACITANCE/LENGTH

5.371987633

APPENDIX VI

This is a listing of three APL functions used to create and analyze by MARTHA the equivalent circuit of the mixer.

A complete example is also given.

```

* LPF59 [0] *
* LPF59 A
* 8-SECTION LOW PASS FILTER IN STRIPLINE SEGMENTS WITH JUNCTION ELEMENTS
[1] MULT*(0.0.0254),1,1,0.0254,1,1,0.0254,1000000000,1,0.0254,1,0.0254,0.0254,1
E 12,1E 12,0.0254
[3] PREV=A
[4] A*MULT=A
[5] S1*TEM A[12],A[1] FORDIEL A[13]
[6] S2*TEM A[9],A[2] FORDIEL A[10]
[7] S3*TEM A[12],A[3] FORDIEL A[13]
[8] S4*TEM A[9],A[4] FORDIEL A[10]
[9] S5*TEM A[12],A[5] FORDIEL A[13]
[10] S6*TEM A[9],A[6] FORDIEL A[10]
[11] S7*TEM A[12],A[7] FORDIEL A[13]
[12] S8*TEM A[9],A[8] FORDIEL A[10]
[13] S9*TEM A[12],A[23] FORDIEL A[13]
[14] L1*L(+0.0254)*LSTEP A[19],A[9],A[18],A[20],A[15]
[15] L2*L(+0.0254)*LSTEP A[14],A[9],A[12],A[20],A[15]
[16] L3*L(+0.0254)*LSTEP A[14],A[16],A[12],A[20],A[15]
[17] L4*L(+0.0254)*LSTEP A[14],A[18],A[12],A[20],A[15]
[18] C1=C(C0*200*A[21])*A[14]-A[17]
[19] C2=C C0*A[14]-A[11]
[20] C3=C C0*A[19]-A[11]
[21] C4=C C0*A[14]-A[19]
[22] J1*(WS L3) WC WP C1*A[22]*2
[23] J2*(WP C2*A[22]*2) WC WS L2
[24] J3*(WS L2) WC WP C2*A[22]*2
[25] J4*(WS L1) WC WP C3
[26] J5*(WP C4) WC WS L4
[27] NET*J1 WC S1 WC J2 WC S2 WC J3 WC S3 WC J2 WC S4 WC J3 WC S5 WC J2 WC S6
[28] NET*NET WC J3 WC S7 WC J2 WC S8 WC J3 WC S9 WC J5
[29] ZNIN*ZG*ZN*A[16]
[30] ZNOUT*ZL*A[18]
[31] PRINT 3 PLACES DB IL,DB S11,DB S22,DEG S11 OF NET
[32] SPLOLPF=NET

```

```

      BS(0)
      BS A
      A EQUIVALENT CIRCUIT OF AN ANTI-PARALLEL DIODE PAIR IN SUBHARMONIC WA
      UEGUIDE MIXER
      F+1000000000 43 44 45 22.8 23.3 23.8 2.6
      S1+WT5 WG(A(7)*1000000000),A(6),(A(1)*0.0254)
      TERM22+WG(A(7)*1000000000),A(6)
      TERM42+R A(8)
      LOLPF+(WP C A(10)*1E-12) WC(WS L A(11)*1E-9) WC(WP C A(12)*1E-12)
      LOLPF+LOLPF WC(WS L A(13)*1E-9) WC(WP C A(14)*1E-12) WC(WS L A(15)*1
      E-9) WC(WP C A(16)*1E-12) WC(WS L A(17)*1E-9)
      WC(WP C A(18)*1E-12)
      LOLPF+LOLPF WC(WS L A(19)*1E-9) WC(WP C A(20)*1E-12)
      S2+TEM A(4),A(9)*0.0254
      LOLPF+SLOLPF
      TERMLO+(S2 WC LOLPF) WT TERM42
      TERMRF+S1 P TERM22
      PARASIT+(WP C A(5)*2E-12) WC(WP R A(3)) S C A(2)*1E-12
      PARASIT+(WP C A(2)*1E-12) WC(WS R A(3)) WC PARASIT
      NET+PARASIT WT TERMLO S TERMRF
      A ZN+250
      ZN+290
      PRINT 3 PLACES Z,DB SC OF NET
      PREV+A
      A
      LONET+LOLPF WC S2 WC(WS TERMRF) WC WN PARASIT
      A RFNET+(WP S1) WC WN PARASIT
      RFNET+(WP S1) WC(WS TERMLO) WC WN PARASIT
      STORED+10
      STORE Z OF NET
      ZJUNC+ZFOF STORED
      A

```

```

V PT [0]V      [34] 4.343xPWR2
V PT U
[1] BS U
[2] F-1000000000x(22.8+0.5x0.12),2.6
[3] A PRINT 2 PLACES H21,MAG H21,G21,MAG G21 OF LONET
[4] A W1+X[1]
[5] A W2+X[2]
[6] A W3+X[3]
[7] A W4+X[4]
[8] A W5+X[5]
[9] EG+1
[10] ZL+1000000000000
[11] ZG+PREV[B]
[12] PWR+VOLT-STORED+10
[13] STORE V2 OF LONET
[14] VOLT+STORED
[15] ZL+0
[16] STORED+10
[17] STORE CG OF LONET
[18] PWR+(VOLT[1;1]xSTORED[1;1])-VOLT[1;2]x(1)xSTORED[1;2]
[19] 1 AVAILABLE POWER RATIO AND DB AT L.O.
[20] PWR
[21] 4.343xPWR
[22] F-1000000000x 43 44 45
[23] ZL+1000000000000
[24] ZG+TERM22
[25] PWR2-VOLT2+STORED+10
[26] STORE V2 OF RFNET
[27] VOLT2+STORED
[28] ZL+0
[29] STORED+10
[30] STORE CG OF RFNET
[31] PWR2+(VOLT2[1;1]xSTORED[1;1])-VOLT2[1;2]x(1)xSTORED[1;2]
[32] 1 AVAILABLE POWER AT DIODES, RATIO AND DB AT R.F.
[33] PWR2

```

PERFORMANCE CRITERIA CALCULATED FOR THE MIXER WITH THE BEST
PERFORMANCE ACHIEVED.

Impedance at the RF port

Frequency (GHz)	Z_{oc} (ohms)	Z_{sc} (ohms)
43	$36 + j 190$	$9.9 + j 0.61$
44	$843 - j 190$	$7.7 + j 0.77$
45	$33 - j 150$	$6.7 + j 2.0$

η_{LO}

Frequency (GHz)	η_{LO}
22.8	0.86
23.3	0.87
23.8	0.85

η_{IF}

Frequency (GHz)	η_{IF}
2.6	0.70

Impedance at the diode terminals

Frequency (GHz)	Z (ohms)
43	$88 + j 31$
RF 44	$118 - j 31$
45	$87 - j 69$
22.8	$11 - j 8.2$
LO 23.3	$13 - j 3.9$
23.8	$18 + j 2.2$
IF 2.6	$72 - j 21$

APPENDIX VII

Test Set-Up & Measurements

The function of the measurement set-up is to provide the mixer under test with two known signals, namely an RF and a LO, and detect the resulting output signal or IF.

Both inputs had to sweep over their required bandwidth as a minimum, i.e., 22.8 to 23.8 GHz for the LO and 43 to 45 GHz for the RF. Furthermore, the sweeping should be synchronous for both inputs in order to maintain the IF output at the single frequency of 2.6 GHz. This was the operational mode of the mixer and the test set-up was made to replicate this mode.

The sweep-synchronization function was simply accomplished by exploiting the FM feature of the Hewlett Packard model 8690 sweeper mainframe. These Backward-Wave-Oscillator (BWO) based sources were used for both LO and RF. The procedure is as follows:

One of the sweepers, say the LO, is in the "AUTO" sweep mode covering the LO band. A "SWEEP OUT" signal is available which is a 0 to 15 Volt voltage ramp proportional to the instantaneous output frequency of the LO BWO. This voltage signal is passed through a simple variable voltage divider and connected to the FM input of the second or RF sweeper. The FM input controls the output frequency of the RF sweeper about its quiescent setting as in a voltage-controlled oscillator with a linear V versus F curve. The purpose of the variable voltage divider is to reduce the 0 to 15 Volt ramp swing to the level required for the RF bandwidth required, i.e., without the divider, a full 15 Volt ramp would cause a full-band RF sweep from 33 to 50 GHz, and typically bandwidths from 42 to 46 GHz were more convenient.

The set-up is outlined in Fig. VII-1. Both input levels are measured using matched waveguide thermistor mounts before the mixer is put in place. Each input has a rotary vane attenuator, frequency meter and a 10 dB directional coupler to measure reflection and match of the inputs into the mixer.

The IF output was measured in power and frequency using a spectrum analyzer or a calibrated crystal detector and an oscilloscope.

Conversion loss, L_c , is determined as the difference between the RF signal power produced by the RF sweeper and the IF power detected. Both LO and RF sliding short tuners could be adjusted for minimum L_c . An oscilloscope display was convenient to show the variations in L_c across the RF band. For this, the horizontal signal would be the "SWEEP OUT" of the LO source and the vertical would be the output of an IF crystal detector.

The result is a trace of IF power at 2.6 GHz versus RF frequency.

One complication arises, however, in that the RF signal input cannot be perfectly leveled, therefore, the IF output will not directly represent conversion loss. An expedient solution is to trace on the scope CRT the "normalized" power line to account for this unflatness and still display a useful picture.

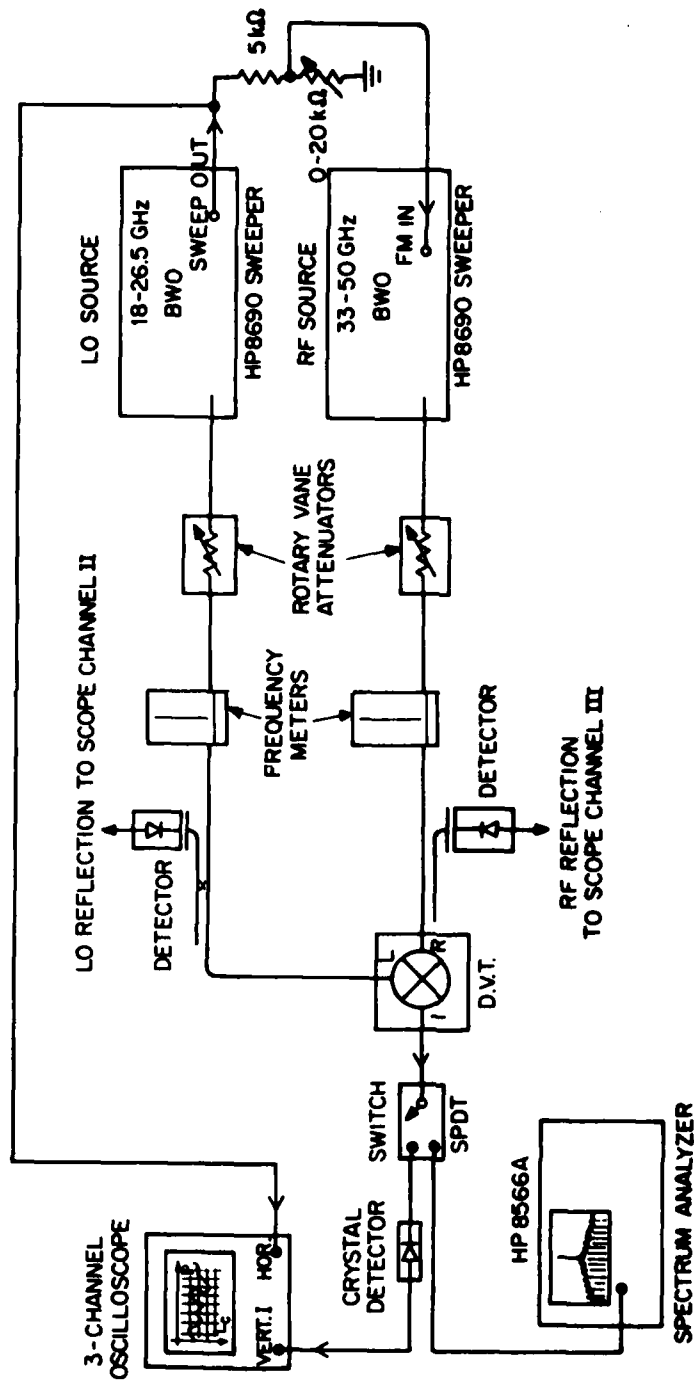
One such photograph is in Fig. VII-2. The crystal detector had a negative polarity so the L_c = infinite base line is at the top. Three normalizing lines are marked corresponding to L_c = 8, 9 and 10 dB bottom to top respectively.

A waveguide band-pass filter was present at the RF input with a 2.3 GHz pass band centered at 44 GHz. Frequency markers are placed at 43 and 45 GHz. The horizontal sweep covers 42 to 46 GHz corresponding to a synchronous LO sweep from 22.3 to 24.3 GHz and a fixed IF of 2.6 GHz. Figure 2 shows L_c to vary between 8.2 and 10.1 dB over the required band. Both LO and RF sliding-short tuners were adjusted for a combination of best L_c and flatness. The reason L_c is 1 dB lower than the 10 ± 1 dB quoted in the text is that +16 to +18 dBm of amplified LO power was available in this experiment compared to the more customary +13 dBm from the BWO alone.

An alternative and more accurate way to measure L_c at a single point in the band is to use a spectrum analyzer and the minimum detectable signal method.* Both ways were in general agreement.

* See for example: HP8566A Operating Manual.

The circuit yielding these results had the best performance achieved. It is thoroughly described in the next appendix.



109491-B

Fig. VII-1. Mixer test set-up.

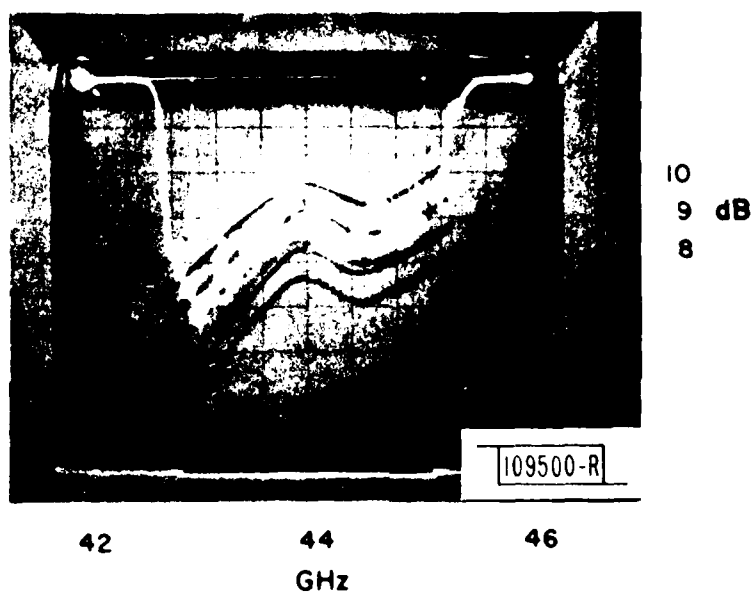


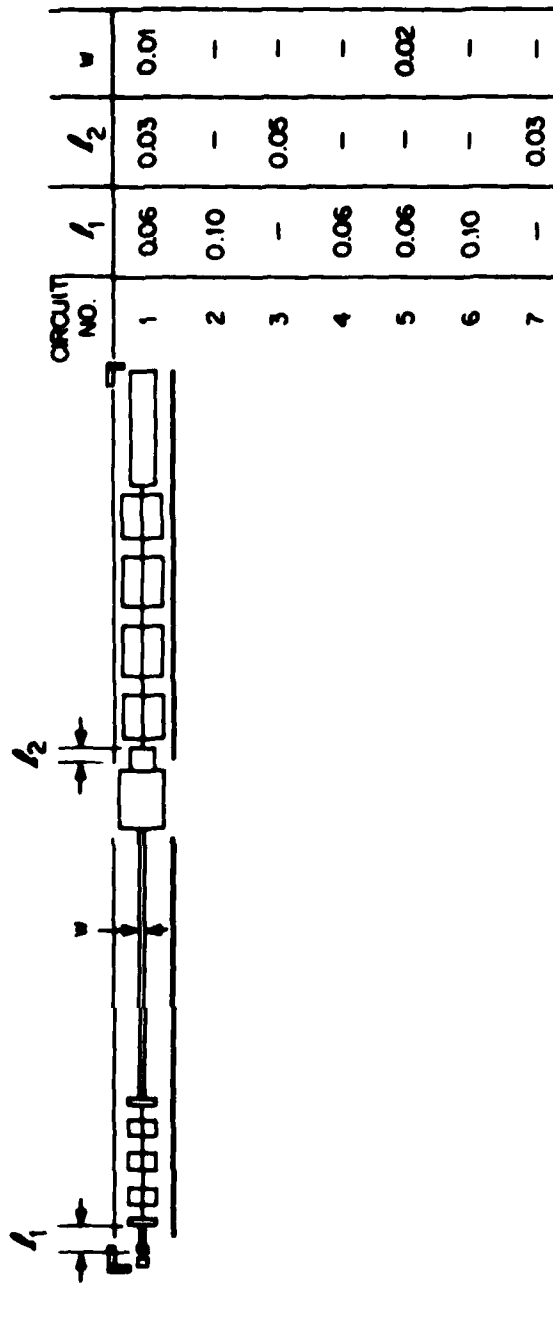
Fig. VII-2. Mixer conversion loss vs frequency.

APPENDIX VIII

Description Of Best Circuit

In Fig. VIII-1 and the following tables, we document the mask called FRONT HALF made by a MANNPLOT pattern generator. The circuit #6 of this mask gave the best performance achieved in this work i.e. $L_c = 10 \pm 1$ dB with +13 dBm LO power or $L_c = 9 \pm .8$ dB with +15 to +18 dBm LO.

The LO waveguide to stripline junction and the IF filter shown in Fig. VIII-1 were designed prior to the development of a program to optimize the junction (see Appendix V). However, the improvement in LO efficiency had that method been used is not fundamental to the mixer proper.



RF
WAVEGUIDE
HEIGHT (0.03in.)

LO
WAVEGUIDE
HEIGHT (0.17in.)

MIXER CIRCUIT MASK

1094 90-B

Fig. VIII-1. Mixer circuit mask.

[illegible]

543.	162.	114.	86.	-847.5	-110.	36.	61.
879.	162.	242.	53.	-694.5	-110.	36.	61.
-495.5	228.	897.	1.	-771.	-110.	39.	61.
-495.5	96.	877.	1.	-329.5	-110.	605.	20.
561.5	228.	877.	1.	38.	-110.	130.	100.
561.5	26.	18.	24.	137.5	-110.	72.	53.
-991.	26.	12.	24.	465.5	-110.	587.	2.
-864.	26.	50.	10.	242.5	-110.	97.	86.
-934.	26.	256.	2.	688.5	-110.	97.	86.
-771.	26.	12.	61.	388.	-110.	114.	86.
-904.	26.	12.	61.	543.	-110.	114.	86.
-638.	26.	36.	61.	879.	-110.	242.	53.
-847.5	26.	36.	61.	-495.5	-44.	897.	1.
-694.5	26.	36.	61.	-495.5	-176.	897.	1.
-771.	26.	39.	61.	561.	-44.	877.	1.
-329.5	26.	605.	10.	561.	-176.	877.	1.
38.	26.	130.	100.	-991.	-246.	18.	24.
137.	26.	72.	53.	-964.	-246.	12.	24.
465.5	26.	587.	2.	-914.	-246.	90.	20.
242.5	26.	97.	86.	-731.	-246.	256.	2.
688.5	26.	97.	86.	-864.	-246.	12.	61.
388.	26.	114.	86.	-598.	-246.	12.	61.
543.	26.	114.	86.	-807.5	-246.	36.	61.
879.	26.	242.	53.	-654.5	-246.	36.	61.
-495.5	92.	897.	1.	-731.	-246.	39.	61.
-495.5	40.	897.	1.	-309.5	-246.	565.	20.
561.5	92.	877.	1.	38.	-246.	130.	100.
561.5	-40.	877.	1.	137.	-246.	72.	53.
-991.	-110.	18.	24.	465.5	-246.	587.	2.
-864.	-110.	12.	24.	242.5	-246.	97.	86.
-934.	-110.	50.	20.	688.5	-246.	97.	86.
-771.	-110.	12.	61.	388.	-246.	114.	86.
-904.	-110.	12.	61.	543.	-246.	114.	86.
-638.	-110.	12.	61.	879.	-246.	242.	53.
				-495.5	-180.	897.	1.

-495.5	1.	897.	1.
561.5	1.	877.	1.
561.5	1.	877.	1.
-991.	24.	18.	24.
-964.	24.	12.	24.
-914.	20.	90.	20.
-731.	2.	256.	2.
-864.	61.	12.	61.
-598.	61.	12.	61.
-807.5	61.	36.	61.
-654.5	61.	36.	61.
-731.	61.	39.	61.
-309.5	20.	565.	20.
38.	100.	130.	100.
127.	53.	52.	53.
445.5	2.	587.	2.
222.5	86.	97.	86.
668.5	86.	97.	86.
368.	86.	114.	86.
523.	86.	114.	86.
869.	53.	262.	53.
-495.5	1.	897.	1.
-495.5	1.	897.	1.
561.5	1.	877.	1.
561.5	1.	877.	1.

END OF FILE REACHED

.save

EDIT:

.

```

sort
ENTER FIRST DIMENSION OF PLATE (2,3,,4 OR 5)FOR 2X2,3X3,4X5,5X5
.3
ENTER X,Y CO-ORDINATES FOR CENTER OF PLATE:
.0.0
ENTER MASK NUMBER OR 'N' IF NONE WANTED:
.N
ENTER UNIQUE PATTERN FILENAME.
.front
MASK COMPLETE? Y OR N:
.Y
TIME - 19. EXPOSURES - 452.
SORT FINISHED, FILE NO. 1 FILENAME:FRONT FILETYPE:E2717

CONSOLE INPUT. ENTER COMMAND PLEASE:

.quit
1 SORTED FILES HAVE BEEN CREATED.
GOODBYE.
R; T-7.91/10.06 14:10:22
.

```

ACKNOWLEDGEMENTS

The assistance of David Reece in assembly and testing is gratefully acknowledged. Many thanks also to William Fielding and his team for their flawless machining.

REFERENCES

1. E. Yamashita, "Stripline with Rectangular Outer Conductor and Three Dielectric Layers," IEEE, Trans. Microwave Theory Tech. MTT, 18, 238 (1970).
2. H. A. Watson ed. Microwave Semiconductor Devices and Their Circuit Applications (McGraw-Hill, New York, 1969).
3. A. A. Saleh, Theory of Resistive Mixers (MIT Press Cambridge, MA, 1971).
4. M. Cohn, J. Degenford et al, "Harmonic Mixing with an Antiparallel Diode Pair," IEEE Trans. Microwave Theory Tech. MTT, 23, 667 (1975).
5. M. Barber, "Noise Figure and Conversion Loss of the Schottky Barrier Mixer Diode," IEEE Trans. Microwave Theory Tech. MTT, 15, 629 (1967).
6. Just-Dietrich Buchs et al., "Frequency Conversion Using Harmonic Mixers with Resistive Diodes," Microwave, Optics and Acoustics 2 71-76 (1978).
7. L. Dickens, "An Integrated-Circuit Balanced Mixer, Image and Sum Enhanced," IEEE Trans. Microwave Theory Tech. MTT, 23, 276 (1975).
8. B. Vowinkel, "Image Recovery Millimeter-Wave Mixer," Ninth European Microwave Conference 1979, pp. 726-730.
9. M. V. Schneider, "Harmonically Pumped Stripline Down-Converter," IEEE Trans. Microwave Theory Tech. MTT, 23, 271 (1975).
10. W. W. Snell et al., "Millimeter-Wave Thin-Film Downconverter," IEEE Trans. Microwave Theory Tech. MTT, 24, 804 (1976).
11. T. F. McMaster, "Millimeter-Wave Receivers with Subharmonic Pump," IEEE Trans. Microwave Theory Tech. MTT, 24, 948 (1976).
12. E. R. Carlson, "Subharmonically Pumped Millimeter-Wave Mixers," IEEE Trans. Microwave Theory Tech. MTT, 26, 706 (1978).
13. A. G. Cardiasmenos et al., "Low Noise Thin Film Downconverters For Millimeter Systems Applications," 1978 International Microwave Symposium Proceedings, pp. 399-401, (New York, 1978).
14. A. G. Cardiasmenos, "New Diodes Cut The Cost Of Millimeter-Wave Mixers," Microwaves 17 78-84 & 86-88 (1978).
15. P. Penfield Jr., MARTHA User's Manual (MIT Press, Cambridge, MA, 1971).

UNCLASSIFIED

SECURITY CLASSIFICATION OF THIS PAGE (When Data Entered)

19 REPORT DOCUMENTATION PAGE		READ INSTRUCTIONS BEFORE COMPLETING FORM
1. REPORT NUMBER 18 ESD-TR-81-196	2. GOVT ACCESSION NO.	3. RECIPIENT'S CATALOG NUMBER
4. TITLE (and Subtitle) EHF Test-Bed Subharmonic Mixer	5. TYPE OF REPORT & PERIOD COVERED 9 Technical Report	
7. AUTHOR(s) 10 Maurice J Aghion 14 TR-5611	6. PERFORMING ORG. REPORT NUMBER Technical Report 567	
9. PERFORMING ORGANIZATION NAME AND ADDRESS Lincoln Laboratory, M.I.T. P.O. Box 73 Lexington, MA 02173	8. CONTRACT OR GRANT NUMBER(s) 15 F19628-80-C-0002	
11. CONTROLLING OFFICE NAME AND ADDRESS Air Force Systems Command, USAF Andrews AFB Washington, DC 20331	10. PROGRAM ELEMENT, PROJECT, TASK AREA & WORK UNIT NUMBERS 16 Program Element No. 63431F Project No. 2929	
14. MONITORING AGENCY NAME & ADDRESS (if different from Controlling Office) Electronic Systems Division Hanscom AFB Bedford, MA 01731	12. REPORT DATE 14 July 1981	
	13. NUMBER OF PAGES 11 82	
	15. SECURITY CLASS. (of this report) Unclassified	
	15a. DECLASSIFICATION DOWNGRADING SCHEDULE	
16. DISTRIBUTION STATEMENT (of this Report) Approved for public release; distribution unlimited.		
17. DISTRIBUTION STATEMENT (of the abstract entered in Block 20, if different from Report)		
18. SUPPLEMENTARY NOTES None		
19. KEY WORDS (Continue on reverse side if necessary and identify by block number) <div style="display: flex; justify-content: space-between;"> <div> mixer harmonic mixer mm wave mixer </div> <div> subharmonic mixing suspended stripline mixer beam-lead diode mixer </div> </div>		
20. ABSTRACT (Continue on reverse side if necessary and identify by block number) <p>The development, design and construction of a subharmonically pumped mixer at 44 GHz using GaAs Schottky beam lead diodes is discussed. A simplified theory is used to derive a three-port equivalent circuit of the complete mixer which includes effects such as diode parasitics and filter characteristics. Specific design criteria are developed at each of the three mixer signal frequencies, RF, LO and IF, which relate this equivalent circuit to the observed performance.</p>		

DD FORM 1 JAN 73 1473 EDITION OF 1 NOV 65 IS OBSOLETE

UNCLASSIFIED

SECURITY CLASSIFICATION OF THIS PAGE (When Data Entered)

317650

DATE
LMED